HHS Public Access

Author manuscript

Circ Res. Author manuscript; available in PMC 2017 April 01.

Published in final edited form as:

Circ Res. 2016 April 1; 118(7): 1062–1077. doi:10.1161/CIRCRESAHA.115.307599.

Disruption of Glut1 in Hematopoietic Stem Cells Prevents Myelopoiesis and Enhanced Glucose Flux in Atheromatous Plaques of *ApoE*$^{-/-}$ Mice

Vincent Sarrazy[1], **Manon Viaud**[1], **Marit Westerterp**[2], **Stoyan Ivanov**[1], **Sophie Giorgetti-Peraldi**[1], **Rodolphe Guinamard**[1], **Emmanuel L Gautier**[3], **Edward B Thorp**[4], **Darryl C. De Vivo**[5], and **Laurent Yvan-Charvet**[1]

[1]Institut National de la Santé et de la Recherche Médicale (INSERM) U1065, Centre Méditerranéen de Médecine Moléculaire (C3M), Atip-Avenir, 06204 Nice, France

[2]Medicine, Division of Molecular Medicine, Columbia University, New York, NY 10032

[3]Institut National de la Santé et de la Recherche Médicale (INSERM) UMR_S 1166, Pierre & Marie Curie University, ICAN Institute of Cardiometabolism & Nutrition, 75006 Paris, France

[4]Pathology, Northwestern University, Feinberg School of Medicine, Chicago, Illinois 60611

[5]Neurology, Columbia University, New York, NY 10032

Abstract

Rationale—Inflamed atherosclerotic plaques can be visualized by non-invasive PET-CT imaging with ^{18}FDG, a glucose analog but the underlying mechanisms are poorly understood.

Objective—Here, we directly investigated the role of Glut1-mediated glucose uptake in *ApoE*$^{-/-}$ mouse model of atherosclerosis.

Methods and Results—We first show that the enhanced glycolytic flux in atheromatous plaques of *ApoE*$^{-/-}$ mice was associated with the enhanced metabolic activity of hematopoietic stem and multi-potential progenitors (HSPCs) and higher Glut1 expression in these cells. Mechanistically, the regulation of Glut1 in *ApoE*$^{-/-}$ HSPCs was not due to alterations in hypoxia-inducible factor 1α (HIF1α) signaling or the oxygenation status of the bone marrow but was the consequence of the activation of the common β subunit of the granulocyte macrophage colony-stimulating factor/interleukin-3 receptor driving glycolytic substrate utilization by mitochondria. By transplanting BM from WT, *Glut1*$^{+/-}$, *ApoE*$^{-/-}$ and *ApoE*$^{-/-}$*Glut1*$^{+/-}$ mice into

Address correspondence to: Dr. Laurent Yvan-Charvet, Institut National de la Santé et de la Recherche Médicale (INSERM) U1065, Centre Méditerranéen de Médecine Moléculaire (C3M), Atip-Avenir, 06204 Nice, France, laurent.yvancharvet@unice.fr.
V.S. and M.V. contributed equally to this study.

Subject Terms:
Animal Models of Human Disease
Lipids and Cholesterol
Growth Factors/Cytokines
Metabolism
Pathophysiology

DISCLOSURES

The authors have declared that no conflict of interest exists.

hypercholesterolemic ApoE deficient mice, we found that Glut1 deficiency reversed $ApoE^{-/-}$ HSPC proliferation and expansion, which prevented the myelopoiesis and accelerated atherosclerosis of $ApoE^{-/-}$ mice transplanted with $ApoE^{-/-}$ BM and resulted in reduced glucose uptake in the spleen and aortic arch of these mice.

Conclusions—We identified that Glut1 connects the enhanced glucose uptake in atheromatous plaques of $ApoE^{-/-}$ mice with their myelopoiesis through regulation of HSPC maintenance and myelomonocytic fate and suggest Glut1 as potential drug target for atherosclerosis.

Keywords

Glucose glycolysis; glucose transporter type 1 (Glut1); hematopoietic stem and progenitor cells (HSPCs); myeloid commitment; atherosclerosis; bone marrow; cholesterol; cell cycling

INTRODUCTION

Atherosclerosis is a chronic, hypercholesterolemia-driven inflammatory disease that is initiated by the deposition of cholesterol-rich lipoproteins in the artery wall, leading to monocyte-macrophage recruitment. Hypercholesterolemia and/or defective cholesterol efflux have also been documented to induce myelopoiesis, which contributes to atherosclerotic lesion formation by fueling plaques with monocytes and neutrophils.[1,2] The monocyte count, in particular, independently predicts risk for coronary artery disease after adjustment for conventional risk factors.[3,4]

Hematopoietic stem cells (HSCs) are quiescent in the bone marrow (BM) niche and are the source of all hematopoietic stem and multi-potential progenitors (HSPCs) and differentiated cells that are critical for the maintenance and replenishment of peripheral leukocytes in adult life, particularly during emergency hematopoiesis. However, we and others have recently shown that chronic cholesterol accumulation in HSPCs due to hypercholesterolemia and/or defective apolipoprotein (Apo)-mediated cholesterol efflux promotes pathogenic HSPC expansion and proliferation leading to uncontrolled myelopoiesis.[5–8] For instance, in the $ApoE^{-/-}$ mouse model of atherosclerosis, the progressive HSPC expansion that drives myelopoiesis,[6] contributed to provide the inflamed atherosclerotic lesions with neutrophils and monocytes.[9–11] Although recent research has focused on elucidating the roles of cytokines and the microenvironment in the proliferation, mobilization and commitment of HSPCs in preclinical model of atherosclerosis,[1,2] the cellular metabolic pathways that regulate these processes remain unknown.

Lessons from various mutant mice displaying a wide range of bioenergetic defects *in vivo* have pointed to a central role for the mitochondrial energy metabolism in HSC stemness.[12–17] Mounting evidence also suggests that HSC quiescence requires a hypoxic environment,[18,19] to maintain glycolysis-biased metabolic activity instead of mitochondrial oxidative phosphorylation (OXPHOS).[20,21] By limiting mitochondrial respiration and ATP production, this could indeed prevent HSCs from producing reactive oxygen species (ROS) to avoid their differentiation and exhaustion.[22–24] In contrast, funneling glucose to the mitochondria for Krebs cycle utilization is required when the HSCs become proliferative or undergo differentiation, most likely due to the high energy demand of these cellular

processes.[21,25] More recently, Oburoglu et al., have also reported that glucose utilization can dictate the myeloid lineage commitment in human HSCs.[26] Intriguingly, increased hematopoietic metabolic activity can be visualized by non-invasive PET-CT imaging with ^{18}FDG, a glucose analog, not only in inflamed atherosclerotic plaques,[27–30] but also in the spleen of patients with cardiovascular diseases,[31,32] reflecting most likely an extramedullary hematopoiesis.[33] However, the relevance of these observations as well as the underlying mechanisms are not fully understood.

In an attempt to better understand the relationship between the enhanced hematopoietic glycolytic activity, HSPC proliferation, myelopoiesis and the development of atherosclerotic lesions, we first showed that an enhanced hematopoietic glycolytic activity in the aortic arch, the BM and the spleen of *ApoE*$^{-/-}$ BM transplanted mice was associated with an enhanced Glut1 expression in *ApoE*$^{-/-}$ HSPCs. Mechanistic studies showed that the up-regulation of Glut1 in *ApoE*$^{-/-}$ HSPCs was not due to an alteration of the oxygenation status of the BM niche but rather was dependent on Ras signaling downstream of the granulocyte macrophage colony-stimulating factor/interleukin-3 receptor driving glycolytic substrate utilization by mitochondria. Finally, we carried out BM transplantation from mice with single or combined deficiencies of ApoE or the glucose transporter Glut1 into *ApoE*$^{-/-}$ mice. Consistent with our hypothesis, *ApoE*$^{-/-}$ mice that had received *ApoE*$^{-/-}$*Glut*$^{+/-}$ BM showed reduced HSPC proliferation and expansion, myelopoiesis and atherogenesis compared to mice that had received *ApoE*$^{-/-}$ BM. Thus, we propose a causal relationship between the enhanced hematopoietic glycolytic activity in *ApoE*$^{-/-}$ mice and their myelopoiesis through regulation of HSPC expansion and fate, offering novel therapeutic perspectives.

METHODS

Materials and additional methods are available in Supplementary material.

Mice and treatments

Glut1$^{+/-}$ mice (kindly provided by Dr. De Vivo, Columbia University) have been crossed to C57BL/6J for more than 12 generations within our colony. *ApoE*$^{-/-}$ (B6.129P2-*Apoe*$^{tm1Unc/J}$), Mx1-cre (B6.Cg-Tg(*Mx1-cre*)$^{1Cgn/J}$) and *HIF1α*$^{fl/fl}$ (B6.129-*Hif1α*$^{tm1Kats/J}$) mice on a C57BL/6J background were obtained from The Jackson Laboratory. *ApoE*$^{-/-}$ (B6.129P2-*Apoe*$^{tm1Unc/J}$) mice expressing Ly5.1 (CD45.2) were crossed to WT mice expressing Ly5.2 (CD45.1) to generate *ApoE*$^{-/-}$ mice expressing Ly5.2 (CD45.1). For each experiment, littermate controls were generated. For the neutralizing antibody experiment, WT and *ApoE*$^{-/-}$ mice were *i.v* injected with IgG control or IL-3Rβ AF549 antibody (R&Dsystems). Animal protocols were approved by the Institutional Animal Care and Use Committee of the French Ministry of Higher Education and Research and the Mediterranean Center of Molecular Medicine (Inserm U1065) and the were undertaken in accordance with the European Guidelines for Care and Use of Experimental Animals. Animals had free access to food and water and were housed in a controlled environment with a 12-h light-dark cycle and constant temperature (22°C).

BM transplantation

BM transplantation was performed as previously described,[5] using BM from 12 to 14 weeks old WT, *Glut1*$^{+/-}$, *ApoE*$^{-/-}$, and *ApoE*$^{-/-}$*Glut1*$^{+/}$ littermates with no significant variation in peripheral leukocyte counts (WT, 6.1±0.5×10^6/mL; *Glut1*$^{+/-}$ 5,6±0.6×10^6/mL; *ApoE*$^{-/-}$ 7.1±0.6×10^6/mL; *ApoE*$^{-/-}$*Glut1*$^{+/-}$ 6,7±0.5×10^6/mL) or BM leukocyte counts (WT, 76±12×10^6; *Glut1*$^{+/-}$ 75±11×10^6; *ApoE*$^{-/-}$ 94±21×10^6; *ApoE*$^{-/-}$*Glut1*$^{+/-}$ 88±16×10^6). Briefly, studies were conducted in 12wks old female *ApoE*$^{-/-}$ mice fed a Western type diet (TD88137) from Harlan Teklad (Madison, WI) for 12wks. Mice were allowed to recover for five weeks after irradiation and BM transplantation before diet studies were initiated. Body weight was recorded at indicated time points. Mice were euthanized in accordance with the American Veterinary Association Panel of Euthanasia. Spleen weights were determined at the time of sacrifice.

Flow cytometry analysis

Blood leukocytes—For identification of peripheral blood leukocytes, 100µl of blood was collected into EDTA tubes before red blood cell lysis (BD Pharm Lyse; BD Biosciences), filtration and staining for 30min on ice. Cells were stained with a cocktail of antibodies against CD45, Ly6C/G, CD115, B220, TCRβ and CD8 as previously described.[5] Briefly, monocytes were identified as CD45$^+$CD115$^+$, neutrophils as CD45$^+$CD115$^-$Ly6C/G^{hi}, B-lymphocytes as CD45$^+$B220$^+$, T-lymphocytes as CD45$^+$TCRβ$^+$ and further subdivided into CD4$^+$, CD8$^+$ and CD8$^+$Ly6C/G$^+$ subsets.

BM HSPCs—BM cells were collected from leg bones, lysed to remove RBCs and filtered before use. Freshly isolated BM cells were stained with the appropriate antibodies for 30min on ice. For haematopoietic subsets, the following lineage antibodies were used: a cocktail of antibodies to lineage committed cells (CD45R, CD19, CD11b, CD3e, Ter-119, CD2, CD4, CD8 and Ly6C/G) and the following stem cell markers: c-Kit, Sca-1, Flt3 (also known as CD135), CD150 (Slamf1), CD34 and FcgRII/III as previously described.[5] Briefly, HSPCs were identified as lin$^-$Sca1$^+$c-Kit$^+$ (LSKs) and HSPC subsets were identified from the most quiescent as long-term LT-HSC (CD34$^-$CD150$^+$Flt3$^-$) to the most cycling as ST-HSC (CD34$^+$CD150$^+$Flt3$^-$) and multipotential progenitors (CD34$^+$CD150$^-$Flt3$^-$ > CD34$^+$CD150$^-$Flt3$^+$). Hematopoietic progenitor cells were identified as common myeloid progenitors (CMP, Lin$^-$Sca1$^-$c-Kit$^+$CD34^{int}FCgRII/III^{int}), granulocyte monocyte progenitors (GMP, Lin$^-$Sca1$^-$c-Kit$^+$CD34^{int}FCgRII/III^{hi}) and megakaryocyte erythrocyte progenitors (MEP, Lin$^-$Sca1$^-$c-Kit$^+$CD34^{lo}FCgRII/III^{lo}). For DNA content analysis, HSPC stained bone marrow cells were fixed in 1% paraformaldehyde in PBS, washed, and stained with 4′,6-diamidino-2-phenylindole (5µg/mL DAPI, Molecular Probes). Cell surface expression of Glut1 was quantified using Glut1 FAB1418 antibody from R&Dsystems or Glut1 RBD ligand (Metafora Biosystems). To assess the uptake of 2-NBDG, prestained cells were incubated with 10 µM 2-NBDG (Invitrogen) for 30 min as previously described.[34] The mitochondrial membrane potential and ROS production were analyzed with 25 nM fluorescent TMRE (AnaSpec) and 5µm CM-H2DCFDA stainings for 30 min on prestained BM cells. In addition, autophagy was monitored in live cells using Cyto-ID autophagy detection kit (Enzo Life Sciences, Lyon, France) according to manufacturer instructions. Viable cells, gated by light scatter or exclusion of CD45$^-$ cells, were analyzed on a four-

laser BD Canto cell analyzer or sorted on a BD FACSAria Cell Sorter both running with DiVa software (BD Biosciences). Data were analyzed using FlowJo software (Tree Star Inc.)

Statistical analysis

Data are shown as mean ± SEM. Statistical significance was performed using Prism t-test or ANOVA were performed according to the dataset. Results were considered as statistically significant when $P<0.05$.

RESULTS

The enhanced glucose uptake in atheromatous plaques under hypercholesterolemic conditions correlates with higher metabolic activity of hematopoietic cells and is associated with higher Glut1 expression in HSPCs

To monitor the metabolic activity of hematopoietic cells, we first investigated the uptake of the radiolabeled D-glucose analogue 2-deoxy [^{14}C] glucose in organs isolated from irradiated *ApoE*$^{-/-}$ recipient mice transplanted with either WT or *ApoE*$^{-/-}$ bone marrow (BM). A more than 2-fold increase in 2-deoxy [^{14}C] glucose uptake was observed not only in the aortic arch of *ApoE*$^{-/-}$ BM transplanted mice compared to controls but also in their BM and spleen (Fig. 1A). An approximately 3.5-fold increase in 2-deoxy [^{14}C] glucose uptake was also consistently observed in colony forming unit assays with the multipotential progenitors (CFU-GEMM) and granulocyte macrophage progenitors (CFU-GM) from the *ApoE*$^{-/-}$ mice (Fig. 1B). The oxygen consumption was 1.3-fold higher in *ApoE*$^{-/-}$ lineage marker-positive (Lin^{+}), *ApoE*$^{-/-}$ Lin^{-} BM cells and Lin^{-}Sca1^{+} progenitors; these cell types represent mature leukocytes or a mix of HSPCs, respectively (Fig. 1C). The higher oxygen consumption seen in *ApoE*$^{-/-}$ cells was most likely maintained by mitochondrial oxygen consumption, as treatment with oligomycin, which inhibits mitochondrial ATP synthase, clearly suppressed their respiration (Fig. 1D). Quantification of the citric acid metabolites by LC-MS showed higher citrate, fumarate and malate but not succinate in *ApoE*$^{-/-}$ leukocytes (Fig. 1E). This was associated with a 1.7-fold increase in succinate dehydrogenase activity in *ApoE*$^{-/-}$ leukocytes (WT, 13.7±1.9. *vs. ApoE*$^{-/-}$, 24.2±4.1 ΔOD/min/mg protein, respectively). Consistent with these findings, an approximately 1.3-fold increase in the mitochondrial membrane potential was observed in *ApoE*$^{-/-}$ Lineage marker-positive (Lin^{+}) and Lin^{-} BM cells by flow cytometry using a fluorescent tetramethylrhodamine ethyl ester (TMRE) dye (Fig. 1F). An analysis of the different populations within the HSPCs showed that the mitochondrial potential of the CD34^{-} long-term hematopoietic stem cells (LT-HSCs) and CD34^{+} HSPCs,[35,36] was increased to the same extent as the Lin^{-} BM cells in the *ApoE*$^{-/-}$ mice (Fig. 1F). This was associated with an increase in reactive oxygen species (ROS) staining in these cells (data not shown). To test whether this phenotype was caused by modulation of the glycolytic pathway in HSPCs, we next used the fluorescent D-glucose analog 2-[N-(7-nitrobenz-2-oxa-1,3-diazol-4-yl)amino]-2-deoxy-D-glucose (2-NBDG) as a tool to examine the glucose uptake in these cells.[34] The NBDG staining was increased by approximately 1.5-fold in the *ApoE*$^{-/-}$ Lin^{+} and Lin^{-} BM cells and CD34^{+} HSPCs, but not in the more primitive fractions of the CD34^{-} LT-HSCs (Fig. 1G). We next assessed the cell surface expression of the glucose transporter 1 (Glut1) in these cells by flow cytometry. An approximately 1.25-fold increase in the Glut1 cell surface expression was observed in the

ApoE$^{-/-}$ Lin^{+} and Lin^{-} BM cells and CD34^{+} HSPCs but not CD34^{-} LT-HSCs (Fig. 1H). This was similar to the NBDG pattern. Together, these observations suggest that the enhanced Glut1 expression and associated glycolytic activity in organs from *ApoE*$^{-/-}$ BM transplanted mice could reflect the metabolic state not only of leukocytes but also HSPCs.

HIF1α is neither involved in the up-regulation of Glut1 in ApoE$^{-/-}$ HSPCs nor the enhanced myelopoiesis of ApoE$^{-/-}$ mice

We next set out to better understand the mechanism leading to Glut1 regulation in the *ApoE*$^{-/-}$ HSPCs. Studies have proposed that the hypoxia inducible factor 1α (HIF1α) up-regulates Glut1,[37] and HIF1α contributes to HSPC homeostasis.[18,20] We first assessed the hypoxic state of the BM cells isolated from irradiated *ApoE*$^{-/-}$ recipient mice transplanted with either WT or *ApoE*$^{-/-}$ BM by flow cytometry with a fluorescein (FITC)-conjugated anti-Pimonidazole (Pimo) antibody at 90 min after intravenous Pimo administration. We did not observe significant changes in Pimo staining in either the *ApoE*$^{-/-}$ Lin^{+} and Lin^{-} BM cells or CD34^{+} HSPCs and CD34^{-} LT-HSCs (Supplemental Fig. IA). HIF1α protein was also barely detectable in WT and *ApoE*$^{-/-}$ BM cell lysates under normoxic culture conditions and cell lysates from *ApoE*$^{-/-}$ BM cells showed amounts of HIF1α protein similar to those of WT cells under hypoxia (Supplemental Fig. IB). Even though, the increase in lactate dehydrogenase A (Ldha) mRNA expression, a HIF1α target gene, upon hypoxia was similar between WT and *ApoE*$^{-/-}$ BM cultures, Glut1 gene expression was higher under both normoxic and hypoxic culture conditions in *ApoE*$^{-/-}$ BM cultures (Supplemental Fig. IC). Thus, to directly test the contribution of HIF1α in the regulation of Glut1-dependent glucose metabolism in *ApoE*$^{-/-}$ HSPC *in vivo*, we next generated an inducible, hematopoietic-specific HIF1αknockout (Mx1-cre *HIF1α*$^{fl/fl}$) on a WT or *ApoE*$^{-/-}$ background. The BM from these mice was transplanted into irradiated *ApoE*$^{-/-}$ mice and after a recovery period, the recipients were then placed on a high fat diet (HFD) for 12 weeks to exacerbate their HSPC expansion (Fig. 2A).[6] HIF1αwas deleted from hematopoietic cells before the start of the diet by sequential polyI:polyC (PIpC) injections, which efficiently excised the HIF1αgene from the BM cells (Fig. 2B and 2C). Ldha mRNA expression was also significantly reduced in the BM of these mice, but Glut1 was only marginally regulated (Fig. 2C). HIF1αdeficiency also did not alter the cell surface expression of Glut1 in CD34^{+} HSPCs and CD34^{-} LT-HSCs (Fig. 2D) or the frequency of these cells (Fig. 2E). Furthermore, quantification of the blood myeloid cells in these mice revealed that HIF1αdeficiency further increased the neutrophil, monocyte and eosinophil counts in these mice (Fig. 2F). Together, these findings suggest that HIF1α does not mediate the upregulation of Glut1 in *ApoE*$^{-/-}$ HSPC or their expansion and minimally contributed to myelopoiesis under hypercholesterolemic conditions.

The IL-3Rβ signaling pathway concomitantly controls the cycling and the up-regulation of Glut1 in ApoE$^{-/-}$ HSPCs

Glut1 can be up-regulated by growth hormone-dependent activation of oncogenes, such as Ras or Src.[38,39] Therefore, we investigated the expression of Glut1 in WT and *ApoE*$^{-/-}$ BM cultures in response to various growth hormones. The Glut1 mRNA levels in WT BM cells were increased upon stimulation with GM-CSF and IL-3, but not Flt3L or TPO, and this response was further increased in the *ApoE*$^{-/-}$ BM cells and blunted by a farnesyl

transferase inhibitor that blocks Ras activation (Supplemental Fig. IIA). These responses were not observed for the HIF1α or Ldha mRNAs (Supplemental Fig. IIA). Flow cytometry analysis confirmed an increase in Glut1 cell surface expression in *ApoE*$^{-/-}$ HSPCs upon IL-3 and GM-CSF stimulation compared to WT HSPCs (Supplemental Fig. IIB). These effects were abrogated by blocking the IL3Rβ signaling pathway and downstream Ras activation with a farnesyl transferase inhibitor, but not by the Jak2 inhibitor, AG490 or the AMP-activated protein kinase (AMPK) activator, metformin (Supplemental Fig. IIB). Removing plasma membrane cholesterol with cyclodextrin also prevented the enhanced Glut1 expression in *ApoE*$^{-/-}$ HSPCs confirming the central role of cholesterol in this regulation (Supplemental Fig. IIB), To directly test the relevance of these observations *in vivo*, an IL3Rβ blocking antibody was next injected into the WT and *ApoE*$^{-/-}$ mice. Consistent with earlier work,[40] we first showed that this antibody efficiently reduced myelopoiesis in the *ApoE*$^{-/-}$ mice and had no effect in WT mice over a 24 h period (Fig. 3A). An analysis of the genes in the glycolytic pathway in the BM cells at the end of the study period revealed no significant changes in the HIF1α or Ldha mRNAs, but the Glut1 mRNA was down-regulated after treatment with the IL3Rβ blocking antibody in the *ApoE*$^{-/-}$ BM (Supplemental Fig. IIC). Quantification of the HSPCs in the BM of these mice by flow cytometry also revealed reduced numbers of CD34^{+} but not CD34^{-} HSPCs in the *ApoE*$^{-/-}$ mice but not the WT mice (Fig. 3B), which correlated with reduced cycling of these cells (Fig. 3C). This was associated with the reduced cell surface expression of Glut1 in the *ApoE*$^{-/-}$ CD34^{+} HSPCs (Fig. 3D). These results revealed that the metabolic requirements for proliferation and expansion of the *ApoE*$^{-/-}$ HSPCs is associated with the IL-3/Glut1 axis and not the HIF1α/Glut1 axis *in vivo*.

Inhibition of mitochondrial glycolytic substrate utilization prevents ApoE$^{-/-}$ HSPC proliferation and myelomonyctic fate in vitro

To determine the contribution of mitochondrial OXPHOS on *ApoE*$^{-/-}$ HSPC proliferation and lineage specification upon IL-3 and GM-CSF treatment, we next artificially suppressed various enzymes that are intricately involved in the regulation of the TCA cycle using pharmacological inhibitors (Fig. 4A). We first validated our *in vitro* BM culture assay by showing that inhibition of the IL-3Rβ signaling pathway (IL3Rβ blocking antibody), inhibition of Ras signaling (farnesyl transferase inhibitor FTI-277) and plasma membrane cholesterol depletion (cyclodextrin CD) prevented *ApoE*$^{-/-}$ HSPC expansion (Fig. 4B) and the generation of CD11b^{+}Gr-1^{+} myeloid cells upon IL-3 and GM-CSF treatment (Fig. 4C). In contrast, inhibition of lactate dehydrogenase (LDH) and acetyl-CoA carboxylase (ACC) using oxamate and Tofa, respectively or activation of AMPK with metformin did not alter *ApoE*$^{-/-}$ HSPC expansion (Fig. 4B) or their myeloid fate (Fig. 4C). Surprisingly, inhibition of mitochondrial respiratory chain complex I with rotenone was also not sufficient to dampen *ApoE*$^{-/-}$ HSPC expansion and myeloid commitment (Fig. 4B and 4C). Given the enhanced succinate dehydrogenase (SDH) activity observed in *ApoE*$^{-/-}$ BM cells, we next evaluated the contribution of the mitochondrial complex II. Inhibition of SDH with 3-nitropropionic acid (3-NPA) specifically prevented the myeloid fate of *ApoE*$^{-/-}$ HSPCs but not their expansion (Fig. 4B and 4C). We next assessed whether inhibition of the conversion of pyruvate for entry to the TCA cycle with a pyruvate dehydrogenase (PDH) inhibitor (CPI-613) and/or a pyruvate carboxylase (PC) inhibitor (chlorothricin) could alter the

expansion and myeloid fate of *ApoE*$^{-/-}$ HSPCs. Although *ApoE*$^{-/-}$ HSPC expansion required both inhibition of PDH and PC (Fig. 4B), their myeloid fate was actually suppressed by inhibiting either PDH or PC (Fig. 4C). This revealed that the conversion of both succinate and pyruvate into the TCA cycle are central metabolic checkpoints for *ApoE*$^{-/-}$ HSPC myeloid lineage specification and to some extent *ApoE*$^{-/-}$ HSPC expansion. Interestingly, the conversion of succinate to fumarate and pyruvate to oxaloacetate (OAA) converge to the malate-aspartate shuttle, known to maximize the number of ATP molecules produced in glycolysis.[41] To address the contribution of this pathway, we suppressed transaminases including glutamate oxaloacetate transaminases (GOTs) using aminooxyacetic acid (AOA). This molecule has been shown to prevent the mitochondria from utilizing glycolytic substrates by inhibiting the malate-aspartate shuttle.[42] Remarkably, treatment with AOA not only prevented *ApoE*$^{-/-}$ HSPC expansion (Fig. 4B) but also their myeloid fate upon IL-3 and GM-CSF treatment (Fig. 4C). These data collectively suggest that mitochondrial metabolic reprogramming of *ApoE*$^{-/-}$ HSPCs is required for their expansion and commitment to the myeloid lineage.

Glut1 mediates the IL-3Rβ-dependent ApoE$^{-/-}$ HSPC proliferation and myelomonyctic fate in vitro

To bolster our observations, we next generated single or combined knockout of ApoE (*ApoE*$^{-/-}$) and Glut1 (*Glut1*$^{+/-}$) mice. The increased oxygen consumption observed in *ApoE*$^{-/-}$ BM cells in response to IL-3 and GM-CSF stimulation was severely reduced by Glut1 deficiency (Fig. 5A). Remarkably, Glut1 deficiency also prevented the enhanced mitochondrial respiration of *ApoE*$^{-/-}$ Lin^{-}Sca1^{+} BM progenitors cultured for 2h after isolation (Fig. 5B). Thus, we next isolated Lin^{-} bone marrow cells (containing predominantly HSPCs) that were placed *in vitro* in medium either alone or supplemented with IL-3 or GM-CSF. We found that Glut1 deficiency led to significantly decreased HSPC expansion either in WT Lin^{-} cultures after IL-3 and GM-CSF stimulation or in *ApoE*$^{-/-}$ Lin^{-} cultures under both unstimulated and stimulated conditions (Fig. 5C and 5D). As a consequence, Glut1 deficiency prevented not only the expansion of the number of cells per well (Supplemental Fig. IID), but also the generation of CD11b^{+}Gr-1^{+} myeloid cells both in response to IL-3 and GM-CSF or in *ApoE*$^{-/-}$ Lin^{-} cultures (Fig. 5E and 5F). This mirrored the ROS production and mitochondrial membrane potential assessed by flow cytometry in HSPCs at the end of the culture period (Fig. 5G and 5H). Mechanistically, we next tested whether Glut1 may mediate the effect of IL-3 on autophagy,[43] since autophagy has recently emerged to regulate HSPC maintenance and a bias toward myelopoiesis.[44,45] Western blot analysis of LC3-II protein levels, an hallmark of autophagy, revealed that Glut1 deficiency prevented the decrease of LC3-II expression in WT and *ApoE*$^{-/-}$ BM cells under basal and IL-3 stimulated conditions (Supplemental Fig. IIIA). To analyze the autophagic flux of HSPCs, we next used the Cyto-ID probe allowing analysis by multicolor flow cytometry. Remarkably, Glut1 deficiency prevented the reduced Cyto-ID staining induced by IL-3 in HSPCs isolated from WT Lin^{-} cultures and restored the autophagic flux of *ApoE*$^{-/-}$ HSPCs to the level of control cells (Supplemental Fig. IIIB and IIIC). These data identify that Glut1 is a key metabolic sensor mediating the growth-regulatory effects of IL-3 through autophagy-dependent modulation of HSPC expansion and myeloid commitment *in vitro*.

Reduced glycolytic activity in mice with hematopoietic Glut1 deficiency prevents ApoE$^{-/-}$ HSPC expansion and proliferation

To directly test the *in vivo* physiological relevance of Glut1 on *ApoE*$^{-/-}$ HSPCs, we transplanted the BM of single or combined knockout of ApoE (*ApoE*$^{-/-}$) and Glut1 (*Glut1*$^{+/-}$) into irradiated *ApoE*$^{-/-}$ mice. After a recovery period, the recipients were placed on a high fat diet (HFD) for 12 weeks using the similar experimental design described earlier (Fig. 6A). At the end of the study period, we confirmed the efficiency of the transplantation procedure by showing an approximately 1.3-fold and 1.5-fold decrease in Glut1 expression in mice receiving *Glut1*$^{+/-}$ or *ApoE*$^{-/-}$*Glut1*$^{+/-}$ BM, respectively using Glut1 antibody and Glut1 RBD ligand by flow cyotmetry (Fig. 6B). An analysis of the different populations within the HSPCs of these mice was next performed (Supplemental Fig. IV). As shown in Figure 1F, low Glut1 cell surface expression was observed in the CD34^{-} LT-HSCs (Fig. 6C and Supplemental Fig. IVD), which were also characterized by CD150^{+} and Flt3^{-} markers (Supplemental Fig. IVA–C).[35,36] Further analysis of the different populations within the HSPCs revealed higher Glut1 expression in the CD34^{+}CD150^{+}Flt3^{-} multi-potent progenitors (MMP2) compared to the CD34^{+}CD150^{-}Flt3^{-} and CD34^{+}CD150^{-}Flt3^{+} multi-potent progenitors (MMP3 and MMP4, respectively)(Fig. 6C). Consistent with these findings, the Glut1 cell surface expression was decreased by an approximately 1.4-fold in the MMP2 of mice receiving either *Glut1*$^{+/-}$ or *ApoE*$^{-/-}$*Glut1*$^{+/-}$ BM (Fig. 6C and Supplemental Fig. IVD). Interestingly, the 2-NBDG staining quantified by flow cytometry suggested Glut1-independent glucose utilization in different populations within the HSPCs, but confirmed an approximately 1.35-fold decrease in 2-NBDG staining in the CD34^{+}CD150^{+}Flt3^{-} MMP2 of mice receiving either *Glut1*$^{+/-}$ or *ApoE*$^{-/-}$*Glut1*$^{+/-}$ BM compared to their respective controls (Fig. 6D and Supplemental Fig. IVE). We next investigated the relationship between the proliferation capacity of the MMP2 and the Glut1-dependent glucose utilization. Although there was no significant decrease in the S/G2M fraction in the CD34^{+}CD150^{+}Flt3^{-} MMP2 and other populations within the HSPCs of mice receiving *Glut1*$^{+/-}$ BM, a significant 1.3-fold decrease in the S/G2M fraction was observed in the CD34^{+}CD150^{+}Flt3^{-} MMP2 and downstream CD34^{+}CD150^{-}Flt3^{-} MMP3 of mice receiving *ApoE*$^{-/-}$*Glut1*$^{+/-}$ BM compared to mice receiving *ApoE*$^{-/-}$ BM (Fig. 6E and Supplemental Fig. IVF). Quantification of the bone marrow HSPCs confirmed an approximately 1.4-fold decrease in the frequency and absolute number of the CD34^{+}CD150^{+}Flt3^{-} MMP2 and downstream MMPs in mice receiving *ApoE*$^{-/-}$*Glut1*$^{+/-}$ BM compared to the controls (Fig. 6F and 6G). Similar findings were also observed in chow-fed *ApoE*$^{-/-}$*Glut1*$^{+/-}$ BM-transplanted mice compared to the *ApoE*$^{-/-}$ BM-transplanted mice (data not shown). Together, these findings reveal that Glut1-dependent glucose utilization was required for *ApoE*$^{-/-}$ MMP2 proliferation and downstream MMP expansion.

Reduced myeloid commitment in ApoE$^{-/-}$ BM with Glut1 deficiency

While working on this manuscript, Pietras et al., elegantly showed that the CD34^{+}CD150^{+}Flt3^{-} MMP2 and downstream CD34^{+}CD150^{-}Flt3^{-} MMP3 exhibited a myeloid-biased multipotential progenitor phenotype.[36] This prompted us to test whether the decreased MMP2 and MMP3 expansion observed in mice receiving *ApoE*$^{-/-}$*Glut1*$^{+/-}$ BM could be associated with a defective myeloid fate specification. The common myeloid progenitor (CMP), granulocyte macrophage progenitor (GMP) and megakaryocyte-erythroid

progenitor (MEP) populations were analyzed by flow cytometry (Supplemental Fig. IVG) and were not significantly reduced in the mice receiving *Glut1*$^{+/-}$ BM despite a trend towards CMPs (Fig. 6H). Nevertheless, the CMP numbers were significantly decreased by more than 1.2-fold in mice receiving *ApoE*$^{-/-}$*Glut1*$^{+/-}$ BM compared to controls receiving *ApoE*$^{-/-}$ BM (Fig. 6H). We noticed that the splenomegaly in the mice receiving the *ApoE*$^{-/-}$ BM was rescued by Glut1 deficiency (Table S1), and the spleen represents an important reservoir of myeloid cells through extramedullary hematopoiesis in *ApoE*$^{-/-}$ mice.[6,33] Therefore, the hematopoietic progenitors were next quantified in this organ. Similar to the BM, we observed a 1.6-fold decrease in the frequency of splenic CMPs in mice receiving *ApoE*$^{-/-}$*Glut1*$^{+/-}$ BM and, to some extent, a 1.3-fold decrease in the percentage of GMPs, but no changes in the MEP population (Fig. 6I). Consistent with these findings, the platelet and red blood cell counts, mean platelet volume (MPV) and hematocrit were unchanged in these mice (Table SI). Peripheral T^{-} and B-cell numbers were also not affected in these mice (Supplemental Fig. VA and VB). In contrast, the blood counts indicated that the leukocytosis, monocytosis, neutrophilia and eosinophilia of mice receiving *ApoE*$^{-/-}$ BM in response to feeding a high fat diet were rescued by Glut1 deficiency (Fig. 6J to 6M). These data indicate that Glut1-dependent glucose utilization is required at the early stage of *ApoE*$^{-/-}$ HSPC commitment to the myeloid lineage.

Glut1 acts in a cell-autonomous fashion to regulate ApoE$^{-/-}$ HSPC proliferation and myelopoiesis

To test whether this phenotype was caused by cell autonomous effects of Glut1 within the myeloid-biased HSPCs or involved a cell extrinsic effect, we performed a competitive BM transplantation experiment with equally mixed BM cells from CD45.1 *ApoE*$^{-/-}$ mice and either CD45.2 *ApoE*$^{-/-}$ BM or CD45.2 *ApoE*$^{-/-}$*Glut1*$^{+/}$ BM into irradiated WT recipients. After BM reconstitution, we found that the frequency of CD45.1 *ApoE*$^{-/-}$ HSPCs, particularly the CD34+ HSPCs, were not affected by the presence of CD45.2 *ApoE*$^{-/-}$*Glut1*$^{+/}$ BM cells, despite the reduced frequency of the CD45.2 *ApoE*$^{-/-}$*Glut1*$^{+/}$ HSPCs (Fig. 7A). These findings mirrored the reduced S/G2M fraction in the CD45.2 *ApoE*$^{-/-}$*Glut1*$^{+/}$ HSPCs without altering the S/G2M fraction in the mixed CD45.1 *ApoE*$^{-/-}$ HSPCs (Fig. 7B). Consistent with these findings on BM HSPCs, there was a preferential accumulation of CD45.1 *ApoE*$^{-/-}$ *vs*. CD45.2 *ApoE*$^{-/-}$*Glut1*$^{+/-}$ blood monocytes and neutrophils (Fig. 7C and 7D), indicative of a cell autonomous proliferative disadvantage of Glut1 deficiency.

Glut1 deficiency prevents the progression of atherosclerosis in ApoE$^{-/-}$ BM-transplanted mice

We next explored the *in vivo* relevance of reducing *ApoE*$^{-/-}$ HSPC proliferation and myelopoiesis through Glut1 deficiency on the development of atherosclerosis. This was tested in *ApoE*$^{-/-}$ recipient mice that received *ApoE*$^{-/-}$ or *ApoE*$^{-/-}$*Glut1*$^{+/-}$ BM fed a high fat diet for 12 weeks (Fig. 6A). As shown in Table S1, the body weight, plasma LDL and HDL cholesterol or plasma glucose were not significantly different with regard to Glut1 deficiency. However, *ApoE*$^{-/-}$ mice receiving *ApoE*$^{-/-}$*Glut1*$^{+/-}$ BM showed an approximately 1.4-fold decrease in the development of atherosclerosis in their proximal aortas (Fig. 8A). Immunohistochemical staining of the aortic root plaques revealed that this

phenotype was associated with a massive decrease in the F4/80^{+} macrophages in the *ApoE*$^{-/-}$*Glut1*$^{+/-}$BM-transplanted mice (Fig. 8B). We also examined the uptake of the radiolabeled D-glucose analog (2-[^{14}C]-DG) after *ex vivo* incubation of the aortic arch and spleen from the *ApoE*$^{-/-}$ mice that received *ApoE*$^{-/-}$ or *ApoE*$^{-/-}$*Glut1*$^{+/-}$ BM. *ApoE*$^{-/-}$*Glut1*$^{+/-}$ BM-transplanted mice showed a significant 1.4-fold and 1.3-fold decrease in total uptake of 2-[^{14}C]-DG in the aortic arch (Fig. 8C) and the spleen (Fig. 8D), respectively compared to controls. We next analyzed Ly6C^{hi} monocyte recruitment into atherosclerotic plaques using fluorescent-labeled latex beads as previously described.[10] Fig. 8E reveals than 2 days after monocyte labeling, there was an approximately 1.8-fold decrease in the number of latex^{+} monocytes in atherosclerotic lesions of *ApoE*$^{-/-}$ mice receiving *ApoE*$^{-/-}$*Glut1*$^{+/-}$ BM compared to mice receiving *ApoE*$^{-/-}$ BM. This reduced recruitment was confirmed by analysis of latex^{+} monocytes in the aortic arch by flow cytometry (Fig. 8F). This paralleled the reduced incorporation of the fluorescent beads in blood monocytes of *ApoE*$^{-/-}$ mice receiving *ApoE*$^{-/-}$*Glut1*$^{+/-}$ BM compared to controls 2 days after labeling (data not shown) reflecting their reduced monocytosis (Fig. 6K). Thus, we showed that Glut1 connects the enhanced glucose uptake in atheromatous plaques of *ApoE*$^{-/-}$ mice,[27–30] with their myelopoiesis through regulation of HSPC maintenance and myelomonocytic fate.

DISCUSSION

Previous studies have shown that inflamed atherosclerotic plaques can be visualized by non-invasive PET-CT imaging with ^{18}FDG, a glucose analog, which correlates with macrophage accumulation and inflammation.[27–30] However, a recent study has called into question the relevance of these observations, as macrophage-specific overexpression of Glut1 did not aggravate atherosclerosis in mice compared to Glut1 sufficient controls,[46] reflecting the need for a better understanding of the underlying mechanisms. Our study provides direct evidence that Glut1 connects the enhanced glucose uptake in atheromatous plaques of *ApoE*$^{-/-}$ mice with their myelopoiesis through Glut1-dependent regulation of HSPC maintenance and myelomonocytic fate.

Recent studies have suggested that HSPC expansion and the associated myelopoiesis could underlie the hypercholesterolemia-induced atherosclerosis in mice.[1,2] However, the rate of ATP generation required for cell proliferation and differentiation cannot be directly explained by cholesterol and requires alternative sources of energy.[47] Our observations indicate that the leukocytes and HSPCs from hypercholesterolemic *ApoE*$^{-/-}$ mice exhibited an increased Glut1-dependent glucose uptake that was associated with increased mitochondrial potential suggesting that the influx of glycolytic metabolites in these cells fuel the mitochondria for oxidative phosphorylation and ATP generation.[21] The low expression of Glut1 in CD34^{-} LT-HSCs compared to other CD34^{+} HSPCs was first counterintuitive, as we initially speculated that the presence of the LT-HSCs in the ‘hypoxic BM niche’ could favor the expression of Glut1 by HIF1α.[37] However, increasing glucose metabolism through translocation of Glut1 to the cell surface is thought to be crucial for the active cells and cell cycle entry rather than quiescence.[48,49] During aerobic respiration, the ATP yield is linked to NAD^{+}-dependent oxidative steps, including oxidative decarboxylation of pyruvate, that requires metabolic shuttle systems to convey reducing equivalents from cytosol to

mitochondria.[41] Our findings indicate that both the oxidative decarboxylation of pyruvate and the transamination reactions of the malate-aspartate shuttle were essential for HSPC expansion and commitment to the myeloid lineage. Thus, it is probably not surprising that we did not observe an accumulation of succinate in *ApoE*$^{-/-}$ BM cultures due to higher succinate dehydrogenase activity favoring fumarate and malate production. The absence of succinate accumulation in *ApoE*$^{-/-}$ BM cells could also contribute to the lack of HIF1α activation in these cells.[50] Consistent with these observations, we did not observe modulation of the oxygenation status of *ApoE*$^{-/-}$ LT-HSCs in chronic hypercholesterolemia, and HIF1α deficiency in WT or *ApoE*$^{-/-}$ hematopoietic cells did not alter Glut1 expression or the HSPC frequency. In fact, HIF1α deficiency in hematopoietic cells rather led to increased myeloid expansion, which could contribute to the role of hypoxia in the development of atherosclerosis.[51] In contrast, and consistent with the alternative regulation of Glut1 by growth hormone-dependent activation of Ras or Src,[38,39] the enhanced Glut1 expression in proliferating *ApoE*$^{-/-}$ HSPCs was prevented by IL3Rβ blockade. This metabolic regulation was critical for the expansion of *ApoE*$^{-/-}$ HSPCs and the associated IL-3-dependent downregulation of autophagy,[43] which is most likely required to limit intracellular lysosomal degradation and fulfill the high-energy demand of these cells for proliferation.

Very recently, increased splenic activity in patients with cardiovascular diseases has been demonstrated by non-invasive PET-CT imaging with ^{18}FDG,[31,32] which could reflect the metabolic activity of extramedullary hematopoiesis required to generates monocytes that infiltrate atherosclerotic plaques.[33] However, these observations do not prove causality. Intriguingly, inhibition of glucose uptake with a 2-deoxyglucose (2-DG) analog has recently ben shown to inhibit myelopoiesis in human HSCs,[26] but the relevance to atherosclerosis has not been tested. The present study clearly establishes that the increased Glut1-dependent glucose utilization in the *ApoE*$^{-/-}$ HSPCs could divert these cells to a myelomonocytic fate leading to extramedullary myelopoiesis and subsequent macrophage deposition-dependent atherosclerotic plaque formation. Indeed, we now provide direct *in vivo* evidence that Glut1 deficiency can significantly reduce the number of CMPs in the *ApoE*$^{-/-}$ BM as well as the number of CMPs and GMPs in the *ApoE*$^{-/-}$ spleen and this was associated with reduced splenic glucose uptake. This led to inhibition of the monocytosis, neutrophilia and eosinophilia in the *ApoE*$^{-/-}$ mice transplanted with the *ApoE*$^{-/-}$ BM. Consistent with the lack of effect of Glut1 deficiency on resting T-cells,[51] we also did not observe variations in the number of lymphocytes in our models. While working on this manuscript, Pietras et al., elegantly showed that the CD34^{+}CD150^{+}Flt3^{-} MMP2, which is now showed to express the most Glut1, and downstream CD34^{+}CD150^{-}Flt3^{-} MMP3 exhibited a myeloid-biased multipotential progenitor phenotype,[36] offering an alternative explanation to the role of Glut1 in favoring myelopoiesis that is independent of a change in other lineage commitments. Together, these findings reveal that the mechanism by which defective ApoE-dependent cholesterol efflux pathways skew hematopoietic stem cells towards myelopoiesis,[5,6] relies on the regulation of Glut1-dependent glucose uptake by the IL-3Rβ signaling pathway.

The metabolic phenotype of *ApoE*$^{-/-}$ HSPCs outlined here could be relevant to the adaptability of HSPCs to cholesterol overload and may indicate that the glycolytic

phenotype of HSPCs is not merely a product of their hypoxic environment. Thus, the existence of different molecular mechanisms underlying the different glycolytic phenotypes in HSPCs may suggest strategies for specifically modulating the pool of HSPCs that are committed to the myeloid lineage under stressed conditions, such as in myeloproliferative disorders,[36] sepsis,[53] myocardium infarction,[54] or chronic atherosclerosis, as shown in the present study. Inhibition of glucose uptake by a Glut1 inhibitor that does not cross the blood-brain barrier could ultimately provide a novel therapeutic approach to prevent myelopoiesis-driven diseases such as atherosclerosis.

Supplementary Material

Refer to Web version on PubMed Central for supplementary material.

Acknowledgments

We thank Dr. Fréderic Labret for assistance with flow cytometry and Dr. Véronique Corcelle for assistance in animal facilities.

SOURCES OF FUNDING

This work was supported by grants to L.Y.C from INSERM ATIP-AVENIR, the Fondation de France (201300038585) and Agence Nationale de la Recherche (ANR).

Nonstandard Abbreviations and Acronyms

2-NBDG	2-[N-(7-nitrobenz-2-oxa-1, 3-diazol-4-yl)amino]-2-deoxy-D-glucose
^{18}FDG	18F-fluorodeoxyglucose
ApoE	Apolipoprotein E
ACC	Acetyl-CoA carboxylase
AMPK	AMP-activated protein kinase
AOA	Aminooxyacetic acid
ATP	Adenosine triphosphate
BM	Bone marrow
CD	Cyclodextrin
CMP	Common myeloid progenitors
CFU-GEMM	Colony forming unit assays with the multipotential progenitors
CFU-GM	Colony forming unit assays with the granulocyte macrophage progenitors
DAPI	4′,6-diamidino-2-phenylindole
DNA	Deoxyribonucleic acid
Flt3L	FMS-like tyrosine kinase 3 ligand
Glut1	Glucose transporter type 1
GM-CSF	Granulocyte macrophage colony-stimulating factor

GMP	Granulocyte monocyte progenitors
GOT	Glutamate oxaloacetate transaminases
HFD	High fat diet
HIF1α	Hypoxia-inducible factor 1α
HSCs	Hematopoietic stem cells
HSPCs	Hematopoietic stem and progenitor cells
IL-3	Interleukin 3
IL-3Rβ	Interleukin-3 receptor βsubunit
LC3	Microtubule-associated protein light chain 3
LC-MS	Liquid chromatography-mass spectometry
LDH	Lactate dehydrogenase
LT-HSC	Long-term hematopoietic stem cells
MEP	megakaryocyte erythrocyte progenitors
MMP	Multi-potent progenitors
mRNA	Messenger RNA
OAA	oxaloacetate
OXPHOS	Oxidative phosphorylation
PET-CT	Positron emission tomography-computed tomography
PBS	Phosphate-buffered saline
PC	Pyruvate carboxylase
PDH	Pyruvate dehydrogenase
Pimo	Pimonidazole
PIpC	polyl:polylC
RBCs	Red blood cells
ROS	Reactive oxygen species
SDH	Succinate dehydrogenase
ST-HSC	Short-term hematopoietic stem cells
TCA	Tricarboxylic acid cycle
TMRE	Tetramethylrhodamine ethyl ester
TPO	Thrombopoietin
WT	Wild-Type

References

1. Swirski FK, Nahrendorf M. Leukocyte behavior in atherosclerosis, myocardial infarction, and heart failure. Science. 2013; 339:161–166. [PubMed: 23307733]
2. Tall AR, Yvan-Charvet L. Cholesterol in inflammation and immune function. Nat Immunol Rev. 2015; 15:104–16.
3. Coller BS. Leukocytosis and ischemic vascular disease morbidity and mortality. Arterioscler Thromb Vasc Biol. 2005; 25:658–670. [PubMed: 15662026]
4. Olivares R, Ducimetière P, Claude JR. Monocyte count: a risk factor for coronary heart disease? Am J Epidemiol. 1993; 137:49–53. [PubMed: 8434572]
5. Yvan-Charvet L, Pagler TA, Gautier EL, Avagyan S, Siry RL, Han S, Welch CL, Wang N, Randolph GJ, Snoeck HW, Tall AR. ATP binding cassette transporters and HDL suppress hematopoietic stem cell proliferation. Science. 2010; 328:1689–1693. (2010). [PubMed: 20488992]
6. Murphy AJ, Akhtari M, Tolani S, Pagler T, Bijl N, Kuo CL, Wang M, Sanson M, Abramowicz S, Welch C, Bochem AE, Kuivenhoven JA, Yvan-Charvet L, Tall AR. ApoE regulates hematopoietic stem cell proliferation, monocytosis, and monocyte accumulation in atherosclerotic lesions in mice. J Clin Invest. 2011; 121:4138–4149. [PubMed: 21968112]
7. Gao M, Zhao D, Schouteden S, Sorci-Thomas MG, Van Veldhoven PP, Eggermont K, Liu G, Verfaillie CM, Feng Y. Regulation of high-density lipoprotein on hematopoietic stem/progenitor cells in atherosclerosis requires scavenger receptor type BI expression. Arterioscler Thromb Vasc Biol. 2014; 34:1900–9. [PubMed: 24969774]
8. Seijkens T, Hoeksema MA, Beckers L, Smeets E, Meiler S, Levels J, Tjwa M, de Winther MPJ, Lutgens E. Hypercholesterolemia-induced priming of hematopoietic stem and progenitor cells aggravate atherosclerosis. The Faseb J. 2014; 28:2202–2213. [PubMed: 24481967]
9. Swirski FK, Libby P, Aikawa E, Alcaide P, Luscinskas FW, Weissleder R, Pittet MJ. Ly-6Chi monocytes dominate hypercholesterolemia-associated monocytosis and give rise to macrophages in atheromata. J Clin Invest. 2007; 117:195–205. [PubMed: 17200719]
10. Tacke F, Alvarez D, Kaplan TJ, Jakubzick C, Spanbroek R, Llodra J, Garin A, Liu J, Mack M, van Rooijen N, Lira SA, Habenicht AJ, Randolph GJ. Monocyte subsets differentially employ CCR2, CCR5, and CX3CR1 to accumulate within atherosclerotic plaques. J Clin Invest. 2007; 117:185–194. [PubMed: 17200718]
11. Drechsler M, Megens RTA, van Zandvoort M, Weber C, Soehnlein O. Hyperlipidemai-triggered neutrophilia promotes early atherosclerosis/clinical perspectives. Circulation. 2010; 122:1837–1845. [PubMed: 20956207]
12. Tothova Z, Kollipara R, Huntly BJ, Lee BH, Castrillon DH, Cullen DE, McDowell EP, Lazo-Kallanian S, Williams IR, Sears C, Armstrong SA, Passegué E, DePinho RA, Gilliand DG. FoxOs are critical mediators of hematopoietic stem cell resistance to physiologic oxidative stress. Cell. 2007; 128:325–339. [PubMed: 17254970]
13. Liu J, Cao L, Chen J, Song S, Lee IH, Quijano C, Liu H, Keyvanfar K, Chen H, Cao LY, Ahn BH, Kumar NG, Rovira II, Xu XL, van Lohuizen M, Motoyama N, Deng CX, Finkel T. Bmi1 regulates mitochondrial function and DNA damage response pathway. Nature. 2009; 459:387–393. [PubMed: 19404261]
14. Gan B, Hu J, Jiang S, Liu Y, Sahin E, Zhuang L, Fletcher-Sananikone E, Colla S, Wang YA, Chin L, DePinho RA. LKB1 regulates quiescence and metabolic homeostasis of hematopoietic stem cells. Nature. 2010; 468:701–704. [PubMed: 21124456]
15. Gurumurthy S, Xie SZ, Alagesan B, Kim J, Yusuf RZ, Saez B, Tzatsos A, Ozsolak F, Milos P, Ferrari F, Park PJ, Shirihai OS, Scadden DT, Bardeesy N. The Lkb1 metabolic sensor maintains haematopoietic stem cell survival. Nature. 2010; 486:659–663. [PubMed: 21124451]
16. Nakada D, Saunders TL, Morrison S. Lkb1 regulates cell cycle and energy metabolism in haematopoietic stem cells. Nature. 2010; 468:653–658. [PubMed: 21124450]
17. Norddahl GL, Pronk CJ, Wahlestedt M, Sten G, Nygren JM, Ugale A, Sigvardsson M, Bryder D. Accumulating mitochondrial DNA mutations drive premature hematopoietic aging phenotypes distinct from physiological stem cell aging. Cell Stem Cell. 2011; 8:499–510. [PubMed: 21549326]

18. Takubo K, Goda N, Yamada W, Iriuchishima H, Ikeda E, Kubota Y, Shima H, Johnson RS, Hirao A, Suematsu M, Suda T. Regulation of the HIF-1α level is essential for hematopoietic stem cells. Cell Stem Cell. 2010; 7:391–402. [PubMed: 20804974]

19. Miharada K, Karlsson G, Rehn M, Rorby E, Siva K, Cammenga J, Karlsson S. Cripto regulates hematopoietic stem cells as hypoxic-niche-related factor through cell surface receptor GRP78. Cell Stem Cell. 2011; 9:330–344. [PubMed: 21982233]

20. Simsek T, Kocabas F, Zheng J, DeBerardinis RJ, Mahmoud AI, Olson EN, Schneider JW, Zhang CC, Sadek HA. The distinct metabolic profile of hematopoietic stem cells reflects their location in a hypoxic niche. Cell Stem Cell. 2010; 7:380–390. [PubMed: 20804973]

21. Takubo K, Nagamatsu G, Kobayashi CI, Nakamura-Ishizu A, Kobayashi H, Ikeda E, Goda N, Rahimi Y, Johnson RS, Soga T, Hirako A, Suematsu M, Suda T. Regulation of glycolysis by Pdk functions as a metabolic checkpoint for cell cycle quiescence in hematopoietic stem cells. Cell Stem Cell. 2013; 12:49–61. [PubMed: 23290136]

22. Jang YY, Sharkis SJ. A low level of reactive oxygen species selects for primitive hematopoietic stem cells that may reside in the low-oxygenic niche. Blood. 2007; 110:3056–3063. [PubMed: 17595331]

23. Miyamoto K, Araki KY, Naka K, Arai F, Takubo K, Yamazaki S, Matsuoka S, Miyamoto T, Ito K, Ohmura M, Chen C, Hosokawa K, Nakauchi H, Nakayama K, Nakayama KI, Harada M, Motoyama N, Suda T, Hirao A. Foxo3a is essential for maintenance of the hematopoietic stem cell pool. Cell Stem Cell. 2007; 1:101–112. [PubMed: 18371339]

24. Chen C, Liu Y, Liu R, Ikenoue T, Guan KL, Liu Y, Zheng P. TSC-mTOR maintains quiescence and function of hematopoietic stem cells by repressing mitochondrial biogenesis and reactive oxygen species. J Exp Med. 2008; 205:2397–2408. [PubMed: 18809716]

25. Yu WM, Liu X, Shen J, Jovanovic O, Pohl EE, Gerson SL, Finkel T, Broxmeyer HE, Qu CK. Metabolic regulation by the mitochondrial phosphatase PTPMT1 is required for hematopoietic stem cell differentiation. Cell Stem Cell. 2013; 12:62–74. [PubMed: 23290137]

26. Oburoglu L, Tardito S, Fritz V, de Barros SC, Merida P, Craveiro M, Mamede J, Cretenet G, Mongellaz C, An X, Kiysz D, Touhami J, Boyer-Clavel M, Battini JL, Dardalhon V, Zimmermann VS, Mohandas N, Gottlieb E, Sitbon M, Kinet S, Taylor N. Glucose and glutamine metabolism regulate human hematopoietic stem cell lineage specification. Cell Stem Cell. 2014; 15:169–184. [PubMed: 24953180]

27. Rogers IS, Tawakol A. Imaging of coronary inflammation with FDG-PET: feasibility and clinical hurdles. Curr Cardiol Rep. 2011; 13:138–144. [PubMed: 21274660]

28. Hag AM, Pedersen SF, Christoffersen C, Binderup T, Jensen MM, Jorgensen JT, Skovgaard D, Ripa RS, Kjaer A. (18)F-FDG PET imaging of murine atherosclerosis: association with gene expresion of key molecular markers. PLoS One. 2012; 7:e50908. [PubMed: 23226424]

29. Lee SJ, Thien Quach CH, Jung KH, Paik JY, Lee JH, Park JW, Lee KH. Oxidized low-density lipoprotein stimulates macrophage 18F-FDG uptake via hypoxia-inducible factor-1a activation through Nox2-dependent reactive oxygen species generation. J Nucl Med. 2014; 55:1699–705. [PubMed: 25214643]

30. Garcia-Garcia HM, Jang IK, Serruys PW, Kovacic JC, Narula J, Fayad Z. Imaging plaques to predict and better manage patients with acute coronary events. Circ Res. 2014; 114:1904–1917. [PubMed: 24902974]

31. Kim EJ, Kim S, Kang DO, Seo HS. Metabolic activity of the spleen and bone marrow in patients with acute myocardial infarction evaluated by 18f-fluorodeoxyglucose positron emission tomographic imaging. Circ Cardiovasc Imaging. 2014; 7:454–60. [PubMed: 24488982]

32. Enami H, et al. Splenic metabolic activity predicts risk of future cardiovascular events: demonstration of a cardiosplenic axis in humans. JACC Cardiovasc Imaging. 2015; 8:121–30. [PubMed: 25577441]

33. Robbins CS, Chudnovskiy A, Rauch PJ, Figueiredo JL, Iwamoto Y, Gorbatov R, Etzrodt M, Weber GF, Ueno T, van Rooijen N, Mulligan-Kehoe MJ, Libby P, Nahrendorf M, Pittet MJ, Weissleder R, Swirski FK. Extramedullary hematopoiesis generates Ly-6C(high) monocytes that infiltrates atherosclerotic lesions. Circulation. 2012; 125:364–74. [PubMed: 22144566]

34. Gautier EL, Westerterp M, Bhagwat N, Cremers S, Shih A, Abdel-Wahab O, Lütjohann D, Randolph GJ, Levine RL, Tall AR, Yvan-Charvet L. HDL and Glut1 inhibition reverse a hypermetabolic state in mouse models of myeloproliferative disorders. J Exp Med. 2013; 210:339–353. [PubMed: 23319699]
35. Weissman IL, Shizuru JA. The origins of the identification and isolation of hematopoietic stem cells, and their capability to induce donor-specific transplantation tolerance and treat autoimmune diseases. Blood. 2008; 112:3543–53. [PubMed: 18948588]
36. Pietras EM, Reynaud D, Kang YA, Carlin D, Calero-Nieto FJ, Leavitt AD, Stuart JM, Gottgens B, Passegué E. Functionally distinct subsets of lineage-biased multipotent progenitors control blood production in normal and regenerative conditions. Cell Stem Cell. 2015; 17:35–46. [PubMed: 26095048]
37. Ebert BL, Firth JD, Ratcliffe PJ. Hypoxia and mitochondrial inhibitors regulate expression of glucose transporter-1 via distinct Cis-acting sequences. J Biol Chem. 1995; 49:29083–29089. [PubMed: 7493931]
38. Flier JS, Mueckler MM, Usher P, Lodish HF. Elevated levels of glucose transport and transporter messenger RNA are induced by ras or src oncogenes. Science. 1987; 235:1492–1495. [PubMed: 3103217]
39. Murakami T, Nishiyama T, Shirotani T, Shinohara Y, Kan M, Ishii K, Kanai F, Nakazuru S, Ebina Y. Identification of two enhancer elements in the gene encoding the type 1 glucose transporter from the mouse which are responsive to serum, growth factor, and oncogenes. J Biol Chem. 1992; 267:9300–6. [PubMed: 1339457]
40. Wang M, Subramanian M, Abramowicz S, Murphy AJ, Gonen A, Witztum J, Welch C, Tabas I, Westerterp M, Tall AR. Interleukin-3/Granulocyte macrophage colony-stimulating factor receptor promotes stem cell expansion, monocytosis, and atheroma macrophage burden in mice with hematopoietic ApoE deficiency. Arterioscler Thromb Vasc Biol. 2014; 34:976–984. [PubMed: 24651678]
41. Dawson AG. Oxidation of cytosolic NADH formed during aerobic metabolism in mammalian cells. Trends Biochem Sci. 1979; 4:171–176.
42. Kauppinen RA, Sihra TS, Nicholls DG. Aminooxyacetic acid inhibits the malate-aspartate shuttle in isolated nerve terminals and prevents the mitochondria from utilizing glycolytic substrates. Biochim Biophys Acta. 1987; 930:173–8. [PubMed: 3620514]
43. Lum JJ, Bauer DE, Kong M, Harris MH, Li C, Lindsten T, Thompson CB. Growth factor regulation of autophagy and cell survival in the absence of apoptosis. Cell. 2005; 120:237–48. [PubMed: 15680329]
44. Mortensen M, Soilleux EJ, Djordjevic G, Tripp R, Lutteropp M, Sadighi-Akha E, Stranks AJ, Glanville J, Knight S, Jacobsen SE, Kranc KR, Simon AK. The autophagy protein Atg7 is essential for hematopoietic stem cell maintenance. J Exp Med. 2011; 208:455–67. [PubMed: 21339326]
45. Rozman S, Yousefi S, Oberson K, Kaufmann T, Benarafa C, Simon HU. The generation of neutrophils in the bone marrow is controlled by autophagy. Cell Death Differ. 2015; 22:445–56. [PubMed: 25323583]
46. Nishizawa T, Kanter JE, Kramer F, Barnhart S, Shen X, Vivekanandan-Giri A, Wall VZ, Kowitz J, Devaraj S, O'Brien KD, Pennathur S, Tang J, Miyaoka RS, Raines EW, Bornfeldt KE. An in vivo test of the hypothesis that glucose in myeloid cells stimulates inflammation and atherosclerosis. Cell report. 2014; 7:356–65.
47. Vander Heiden MG, Cantley LC, Thompson CB. Understanding the Warburg effect: the metabolic requirements of cell proliferation. Science. 2009; 324:1029–1033. [PubMed: 19460998]
48. DeBerardinis RJ, Lum JJ, Hatzivassiliou G, Thompson CG. The biology of cancer: Metabolic reprogramming fuels cell growth and proliferation. Cell Metab. 2008; 7:11–20. [PubMed: 18177721]
49. Lunt SY, Vander Heiden MG. Aerobic glycolysis: Meeting the metabolic requirements of cell proliferation. Annu Rev Cell Dev Biol. 2011; 27:441–64. [PubMed: 21985671]

50. Selak MA, Armour SM, MacKenzie ED, Boulahbel H, Watson DG, Mansfield KD, Pan Y, Simon MC, Thompson CB, Gottlieb E. Succinate links TCA cycle dysfunction to oncogenesis by inhibiting HIF-alpha prolyl hydroxylase. Cancer Cell. 2005; 7:77–85. [PubMed: 15652751]

51. Parathath S, Yang Y, Mick S, Fisher EA. Hypoxia in murine atherosclerotic plaques and its adverse effects on macrophages. Trends Cardiovasc Med. 2013; 23:80–4. [PubMed: 23375596]

52. Macintyre AN, Gerriets VA, Nichols AG, Michalek RD, Rudolph MC, Deoliveira D, Anderson SM, Abel ED, Chen BJ, Hale LP, Rathmell JC. The glucose transporter Glut1 is selectively essential for CD4 T cell activation and effectyor function. Cell Metab. 2014; 20:1–12. [PubMed: 24988453]

53. Weber GF, Chousterman BG, He S, Fenn AM, Nairz M, Anzai A, Brenner T, Uhle F, Iwamoto Y, Robbins CS, Noiret L, Maier SL, Zonnchen T, Rahbari NN, Scholch S, Klotzsche-von Ameln A, Chavakis T, Weitz J, Hofer S, Weigand MA, Nahrendorf M, Weissleder R, Swirski FK. Interleukin-3 amplifies acute inflammation and is a potential therapeutic target in sepsis. Science. 2015; 347:1260–5. [PubMed: 25766237]

54. Dutta P, Sager HB, Stengel KR, Naxerova K, Courties G, Saez B, Silberstein L, Heidt T, Sebas M, Sun Y, Wojtkiewicz G, Feruglio PF, King K, Baker JN, van der Laan AJ, Borodovsky A, Fitzgerald K, Hulsmans M, Hoyer F, Iwamoto Y, Vinegoni C, Brown D, Di Carli M, Libby P, Hiebert SW, Scadden DT, Swirski FK, Weissleder R, Nahrendorf M. Myocardial infarction activates CCR2+ hematopoietic stem and progenitor cells. Cell Stem Cell. 2015; 16:477–487. [PubMed: 25957903]

Novelty and Significance

What Is Known?

- Increased hematopoietic metabolic activity can be visualized by non-invasive PET-CT imaging with ^{18}FDG, a glucose analog, not only in inflamed atherosclerotic plaques but also in the spleen of patients with cardiovascular diseases.
- Increased glucose metabolism is thought to be crucial for cellular proliferation, but direct evidence of its role in hematopoiesis is lacking.

What New Information Does This Article Contribute?

- The induction of Glut1 in *ApoE*$^{-/-}$ hematopoietic stem and progenitor cells is the consequence of the growth-regulatory effects of IL-3 and GM-CSF driving glycolytic substrate utilization by mitochondria.
- Deletion of the *Glut1* gene limits the enhanced glycolytic and mitochondrial activity of *ApoE*$^{-/-}$ hematopoietic stem and progenitor cells, attenuating the high-energy demand of these cells for proliferation and expansion and preventing the development of atherosclerosis.
- These findings suggest the presence of proatherogenic crosstalk between nutritional and growth factor signaling pathways in hematopoietic stem and progenitor cells.

The enhanced metabolic activity visualized by non-invasive PET-CT imaging with ^{18}FDG, a glucose analog, in inflamed atherosclerotic plaques and spleen of patients with cardiovascular diseases suggests a link between hematopoietic activity and atherosclerosis. We evaluated this hypothesis by investigating the contribution of Glut1 in the hematopoietic compartment to the development of atherosclerosis in *ApoE*$^{-/-}$ mice. We found that hematopoietic Glut1 deficiency decreased atherosclerosis by preventing hematopoietic stem and progenitor cell proliferation, myelopoiesis and the recruitment of myeloid cells in atherosclerotic lesions independent of plasma lipid profile. In *ApoE*$^{-/-}$ hematopoietic stem and progenitor cells, Glut1 serves as a key metabolic sensor for the high-energy demand of these cells for proliferation favoring glycolytic substrate utilization by mitochondria. These results provide direct evidence showing that 1) Glut1 connects the enhanced glucose uptake in atheromatous plaques and spleen of *ApoE*$^{-/-}$ mice with their myelopoiesis and 2) the activation of Glut1 in hematopoietic stem and progenitor cells of preclinical model of atherosclerosis is proatherogenic. Thus, inhibition of glucose uptake by a Glut1 inhibitor that does not cross the blood-brain barrier may be useful in the treatment of atherosclerosis.

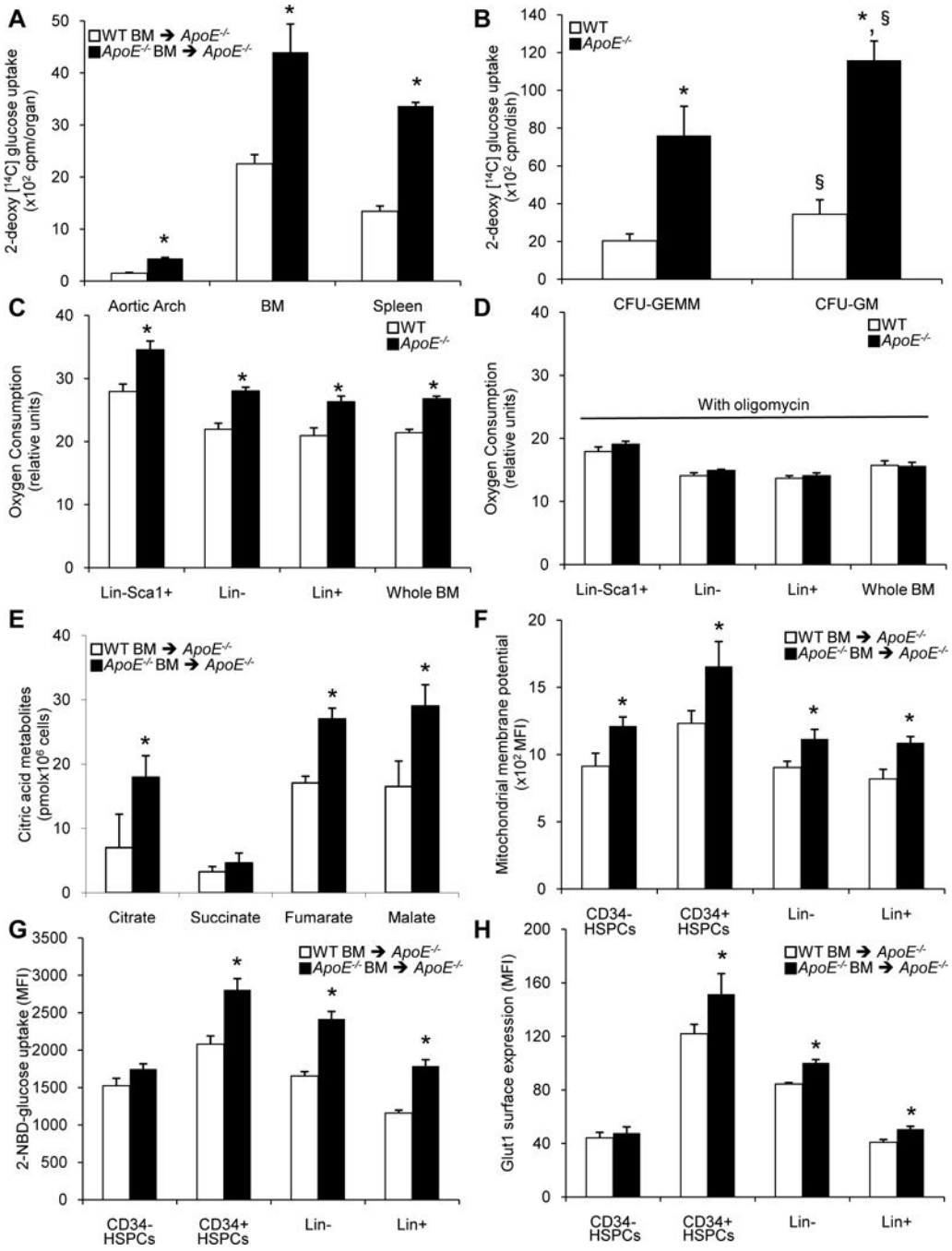

Figure 1. Enhanced glucose utilization in the aortic arch, splenocytes, BM and HSPCs of *ApoE*$^{-/-}$ BM chimeras

(A) 2-deoxy-[^{14}C]-glucose uptake in aortic arch, bone marrow and spleen of *ApoE*$^{-/-}$ recipients transplanted with WT or *ApoE*$^{-/-}$ BM at 12 weeks after the transplantation procedure. **(B)** 2-deoxy-[^{14}C]-glucose uptake was also determined in colony forming unit assays of multipotential progenitors (CFU-GEMM) and granulocyte macrophage progenitors (CFU-GM) from the BM of WT and *ApoE*$^{-/-}$ mice. **(C)** Oxygen consumption of whole BM cells, lineage marker (Lin)$^{+}$, Lin^{-} BM cells and Lin^{-}Sca1^{+} progenitors isolated

from the BM of WT and *ApoE*$^{-/-}$ mice in absence or **(D)** in presence of oligomycin treatment. **(E)** The citric acid metabolites were determined by LC-MS in BM cells isolated from *ApoE*$^{-/-}$ recipients transplanted with WT or *ApoE*$^{-/-}$ BM at 12 weeks after the transplantation procedure. **(F)** The mitochondrial membrane potential (MMP) was measured by flow cytometry using a fluorescent tetramethylrhodamine ethyl ester (TMRE) dye in Lin^{-}, Lin^{+} and CD34^{-} or CD34^{+} HSPCs isolated from the BM of these mice. **(G)** NBD-glucose binding and/or uptake and **(H)** cell surface expression of Glut1 was also quantified in these cells. All results are the means ± SEM and are representative of at least one experiment performed with 6–10 animals per group. **P*<0.05 *vs.* WT. §*P*<0.05 *vs.* the untreated condition.

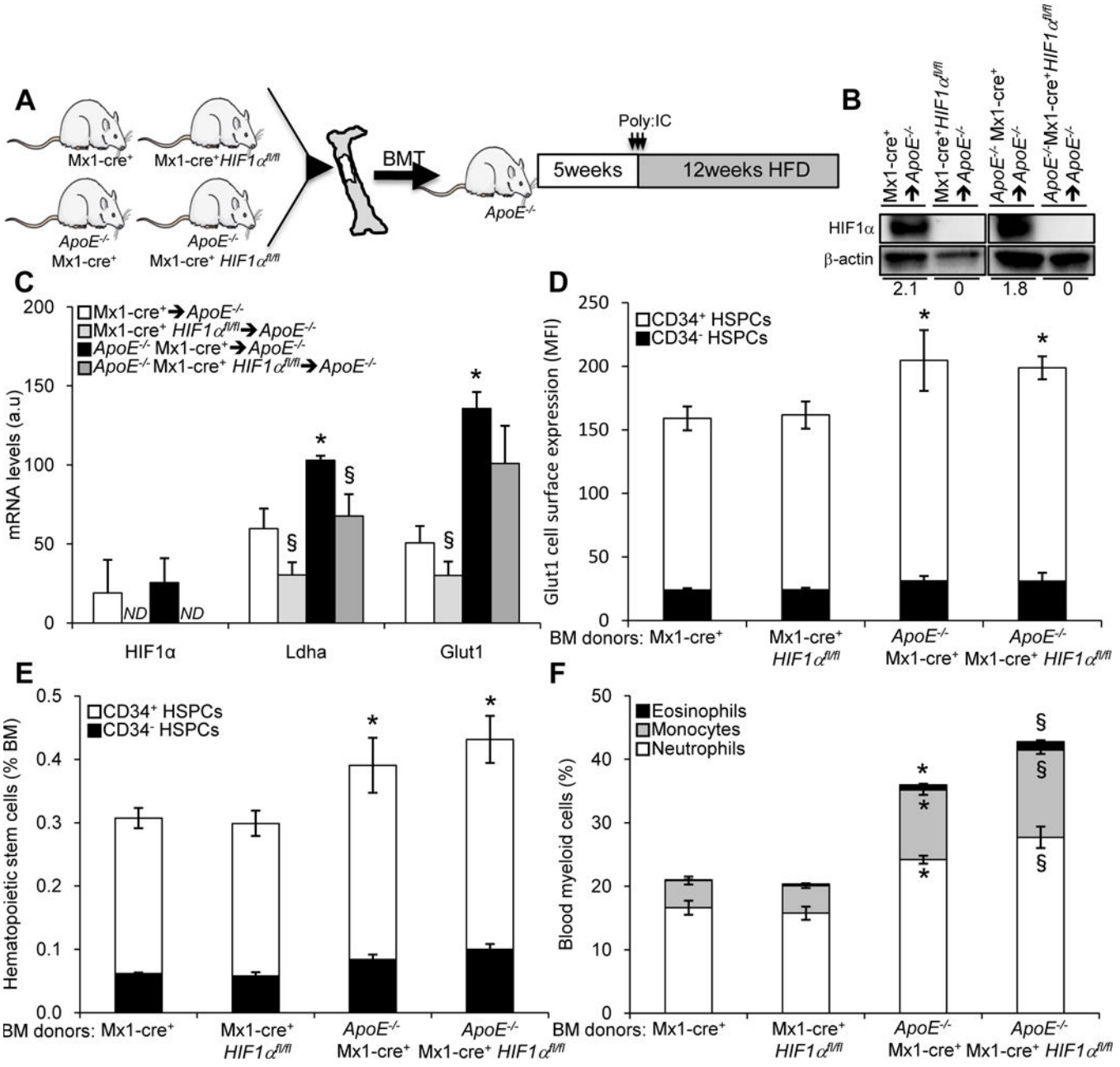

Figure 2. HIF1α-independent regulation of Glut1 expression and *ApoE*$^{-/-}$ HSPC expansion and myeloid lineage fate

(A) Experimental overview. Bone marrow from Mx1-Cre (controls), Mx1-cre *HIF1α*$^{fl/fl}$, *ApoE*$^{-/-}$ Mx1-Cre, *ApoE*$^{-/-}$ Mx1-cre *HIF1α*$^{fl/fl}$ mice were transplanted into *ApoE*$^{-/-}$ recipient mice and, after a 5 week recovery period, the mice were injected with Poly:IC and fed a high fat diet for 12 weeks to induce the expansion of HSPCs. **(B)** Representative Western blots showing HIF1α levels in BM cells freshly isolated from these mice at the end of the study period. Quantification (normalized to β–actin) is expressed as arbitrary unit and indicated by numbers below **(C)** mRNA expression of HIF1α and HIF1α target genes Ldha and Glut1 in BM cells freshly isolated from these mice at the end of the study period. **(D)**

Histograms showing Glut1 cell surface expression (expressed as the mean fluorescence intensity (MFI)) in $CD34^-$ and $CD34^+$ HSPCs. **(E)** Quantification of the $CD34^-$ or $CD34^+$ HSPCs by flow cytometry was expressed as the percentage of total BM. **(F)** peripheral blood neutrophils, monocytes and eosinophils were also quantified in these mice at the end of the study period. The results are the means ± SEM of 6–10 animals per group. $^*P<0.05$ *vs. Mx1-Cre*. $^{\S}P<0.05$ *vs.* $ApoE^{-/-}$ *Mx1-Cre*.

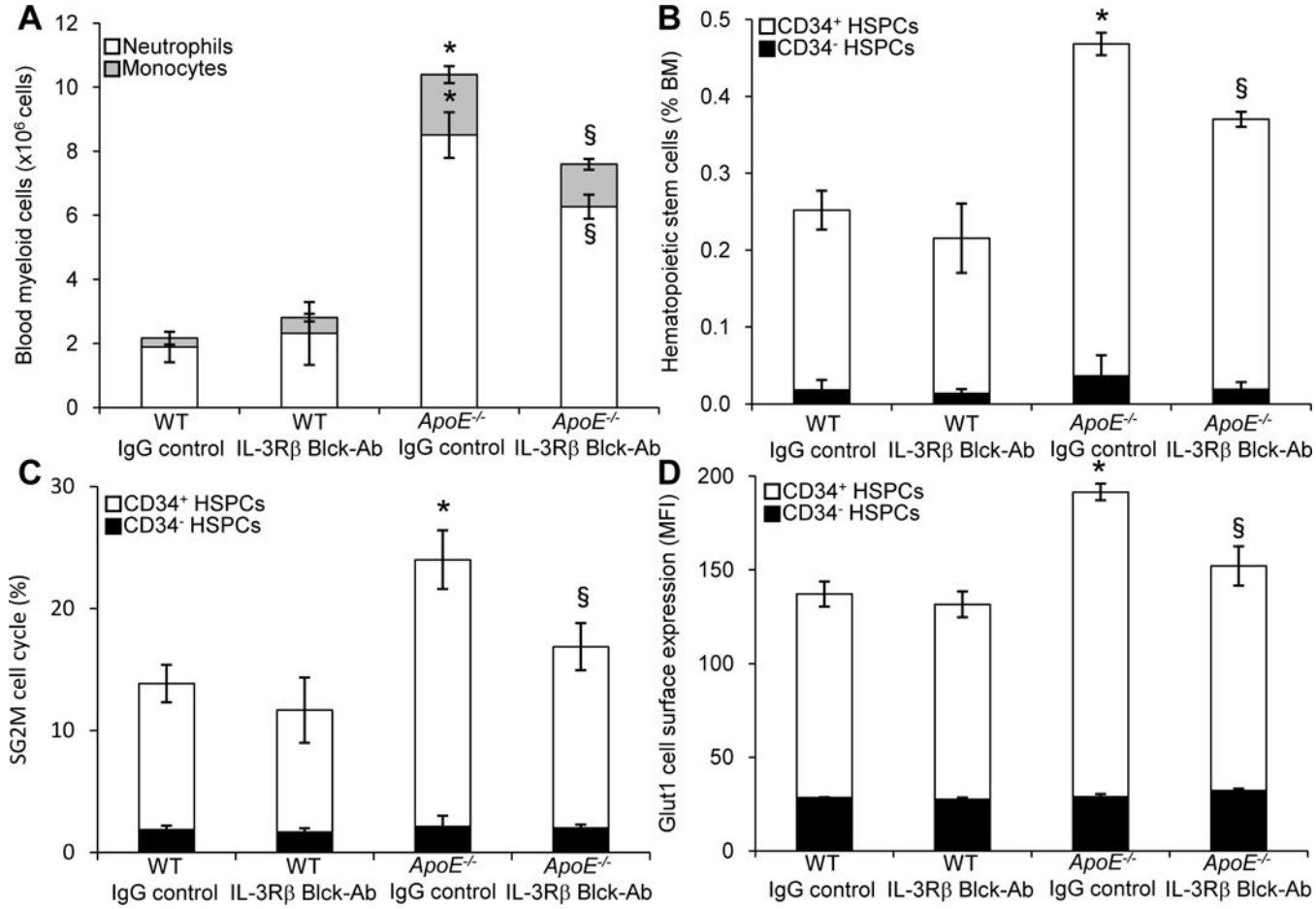

Figure 3. The *ApoE*$^{-/-}$ HSPC expansion and myeloid lineage fate and Glut1 upregulation are driven by the IL3Rβ signaling pathway

(A) Twenty-week-old WT and *ApoE*$^{-/-}$ mice were injected with IgG control or 100μg of the IL-3Rβ blocking antibody for 24 h and analyzed for peripheral blood myeloid cells by flow cytometry. **(B)** The CD34^{-} or CD34^{+} HSPCs were quantified in the BM of these mice and was expressed as the percentage of total BM. **(C)** The percentage of these cells in S/G2M phase was determined by Hoechst staining, and **(D)** Glut1 cell surface expression was expressed as the mean fluorescence intensity (MFI). The results are the means ± SEM of 5 to 6 animals per group. *P<0.05 *vs.* WT IgG control. §P<0.05 *vs. ApoE*$^{-/-}$ IgG control.

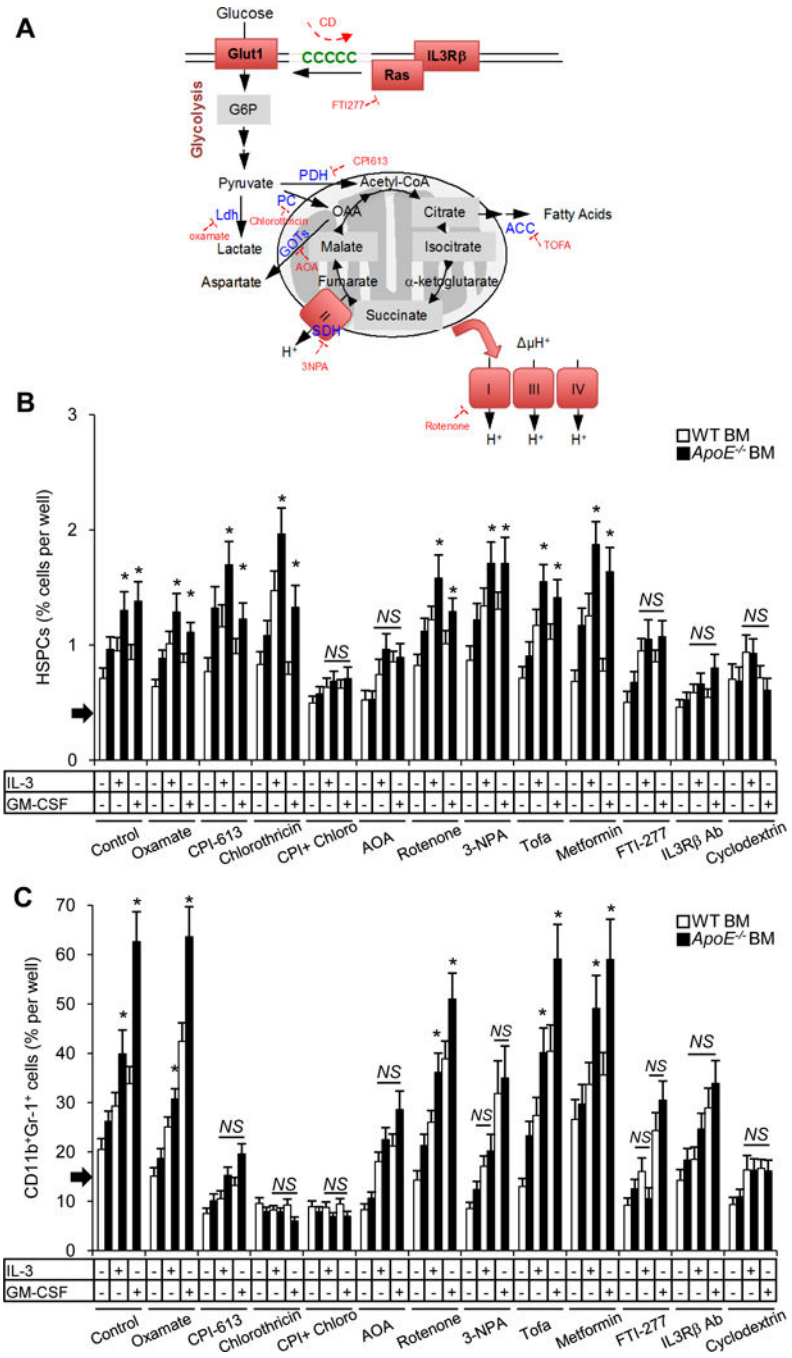

Figure 4. Mitochondrial glycolytic substrate utilization is required for *ApoE*$^{-/-}$ HSPC proliferation and myelomonyctic fate *in vitro*

(A) Schematic representation of the metabolic pathways analyzed using pharmacological inhibitors with key enzymes indicated in blue, inhibitors in red, metabolites in black and cholesterol in green. Red boxes also indicated key signaling molecules. Bone marrow cells from fluorouracil-treated WT and *ApoE*$^{-/-}$ mice were grown for 72h in liquid culture containing 10% FBS IMDM in the presence of the indicated chemical compounds and 6ng/mL IL-3 or 2ng/mL GM-CSF. **(B)** Quantification of HSPCs and **(C)** CD11b^{+}Gr-1^{+}

myeloid cells after *in vitro* culture. Arrows on the y-axis indicate the starting percentage of cells per well before culture. The results are the means ± SEM of an experiment performed with 4 animals per group. $P<0.05$, genotype effect. *NS*, non-significant.

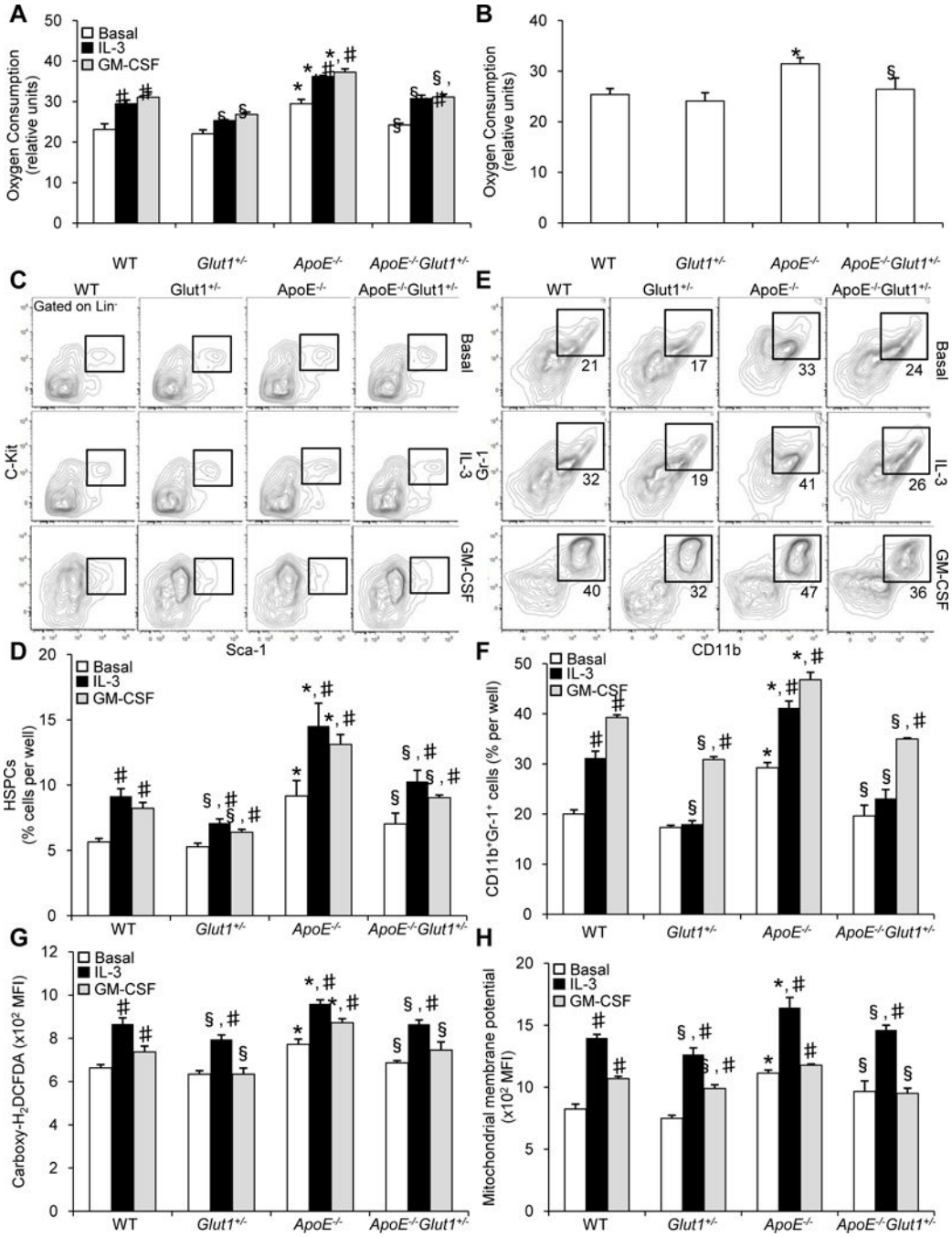

Figure 5. Glut1 is required *in vitro* for the IL3Rβ-dependent *ApoE*$^{-/-}$ HSPC expansion and myeloid lineage fate

(A) Oxygen consumption of WT, *Glut1*$^{+/-}$, *ApoE*$^{-/-}$, and *ApoE*$^{-/-}$*Glut1*$^{+/-}$ BM cells cultured for 48h in presence or absence of 6ng/mL IL-3 or 2ng/mL GM-CSF or **(B)** WT, *Glut1*$^{+/-}$, *ApoE*$^{-/-}$, and *ApoE*$^{-/-}$*Glut1*$^{+/-}$ Lineage marker (Lin) $^{-}$Sca1^{+} progenitors cultured for 2h after isolation. Bone marrow cells from WT, *Glut1*$^{+/-}$, *ApoE*$^{-/-}$, and *ApoE*$^{-/-}$*Glut1*$^{+/-}$ mice were sorted for Lin^{-} cells (i.e, enriched in HSPCs) and cultured for 72h in liquid culture in presence or absence of 6ng/mL IL-3 or 2ng/mL GM-CSF. **(C)** Representative dot

plots and **(D)** quantification of HSPCs after *in vitro* culture. **(E)** Representative dot plots and **(F)** quantification of $CD11b^{+}Gr\text{-}1^{+}$ myeloid cells after *in vitro* culture. **(G)** Quantification of ROS generation and **(H)** mitochondrial membrane potential (MMP) by flow cytometry using fluorescent carboxy-H_2DCFDA and tetramethylrhodamine ethyl ester (TMRE) dyes, respectively in HSPCs after *in vitro* culture. The results are the means ± SEM of n=4 per group. $^{*}P<0.05$, genotype effect. $^{\S}P<0.05$, Glut1-dependent effect. $^{\#}P<0.05$, growth hormone effect.

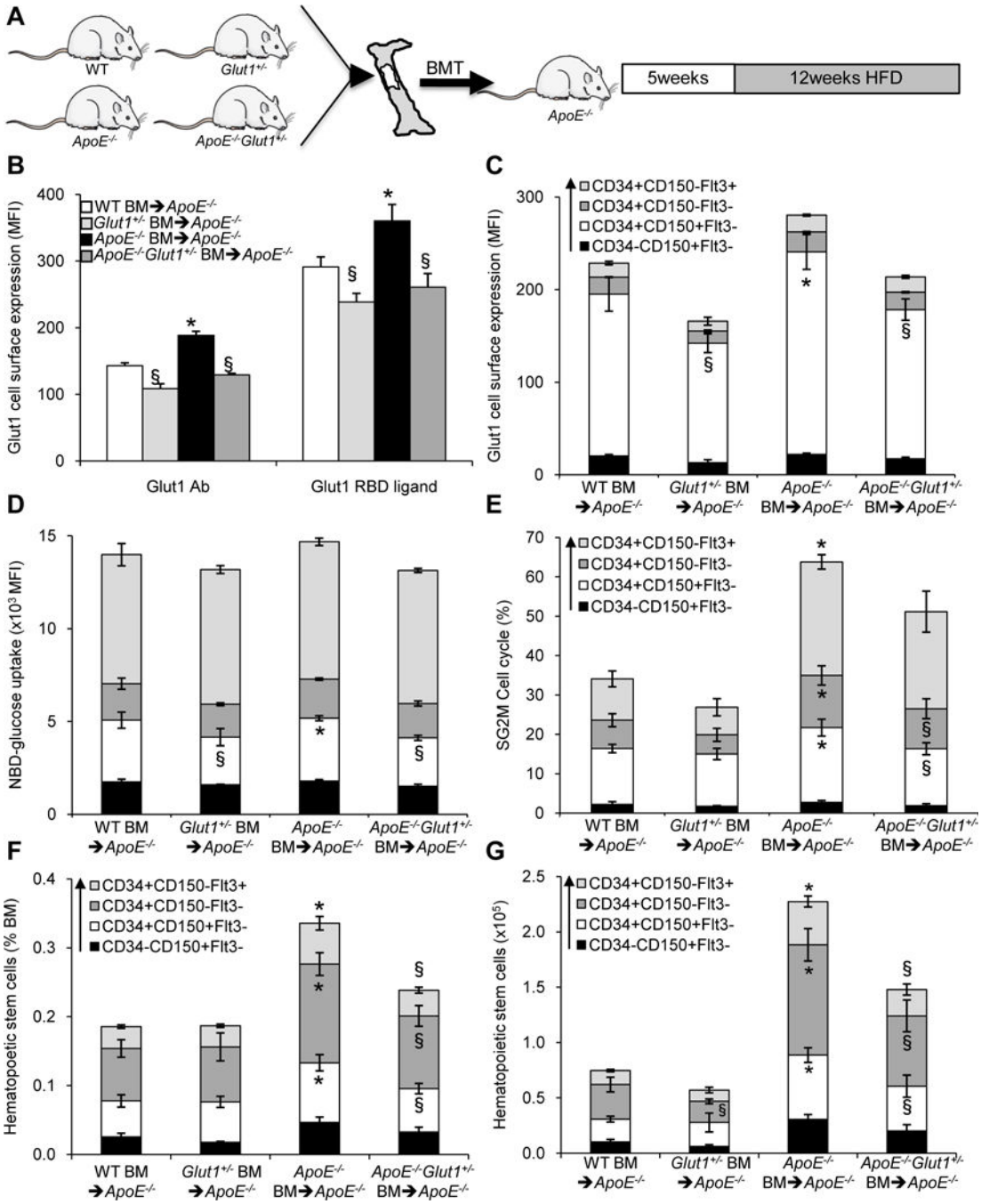

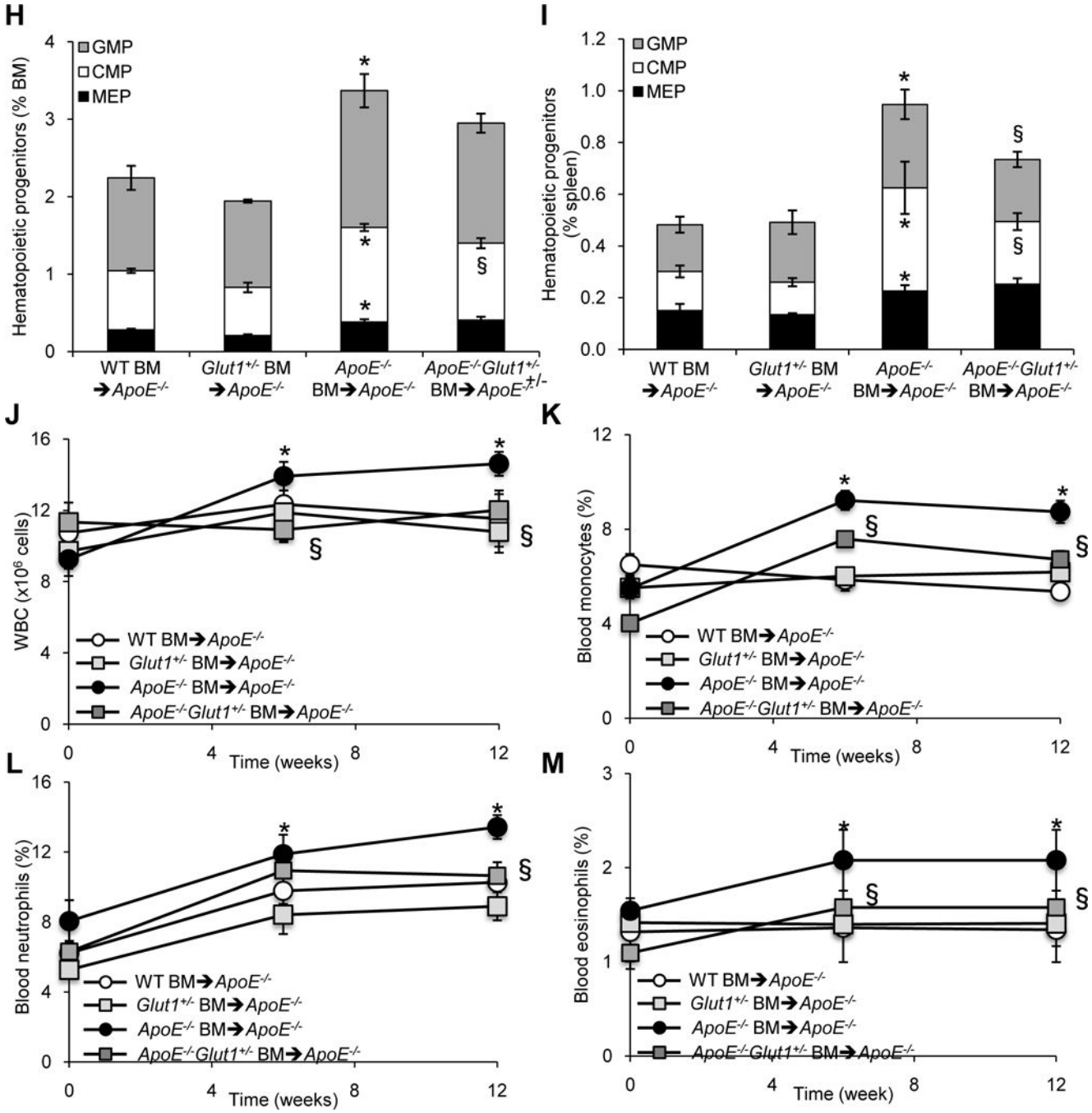

Figure 6. Glut1-dependence of *ApoE*$^{-/-}$ HSPC expansion and myelopoiesis *in vivo*

(A) Experimental overview. Bone marrow from WT, *Glut1*$^{+/-}$, *ApoE*$^{-/-}$, and *ApoE*$^{-/-}$*Glut1*$^{+/-}$ mice were transplanted into *ApoE*$^{-/-}$ recipient mice and, after a 5 week recovery period, the mice were fed a high fat diet for 12 weeks to induce the expansion of HSPCs. **(B)** Glut1 cell surface expression was assessed by flow cytometry in the BM of these mice using Glut1 antibody and Glut1 RBD ligand. Histograms show **(C)** the Glut1 cell surface expression and **(D)** NBD-glucose binding and/or uptake in HSPC subpopulations from the most quiescent (long-term LT-HSCs) to the most cycling multipotential progenitors

($CD34^{-}CD150^{+}Flt3^{-}$>$CD34^{+}CD150^{+}Flt3^{-}$>$CD34^{+}CD150^{-}Flt3^{-}$>$CD34^{+}CD150^{-}Flt3^{+}$) and are expressed as the mean fluorescence intensity (MFI). **(E)** The percentage of cells in S/G2M phase was determined by DAPI staining and flow cytometry, Quantification of HSPC subpopulations expressed as **(F)** percentage of total BM or **(G)** absolute numbers. Histograms showing the quantification of granulocyte macrophage progenitor (GMP), common myeloid progenitor (CMP) and megakaryocyte-erythroid progenitor (MEP) populations are expressed as percentage of **(H)** total BM or **(I)** spleen. Quantification of **(J)** the peripheral blood leukocytes, **(K)** monocytes, **(L)** neutrophils and **(M)** eosinophils over the course of a 12-week high fat diet period. The data are the means ± SEM and are representative of an experiment performed with n=6 (WT and $Glut1^{+/-}$ BM transplanted into $ApoE^{-/-}$ recipients) or n=10–12 ($ApoE^{-/-}$ *and* $ApoE^{-/-}Glut1^{+/-}$ BM transplanted into $ApoE^{-/-}$ recipients) animals per group. *P<0.05 *vs.* $ApoE^{-/-}$ *mice* receiving WT BM. §P<0.05 *vs.* $ApoE^{-/-}$ mice receiving $ApoE^{-/-}$ BM.

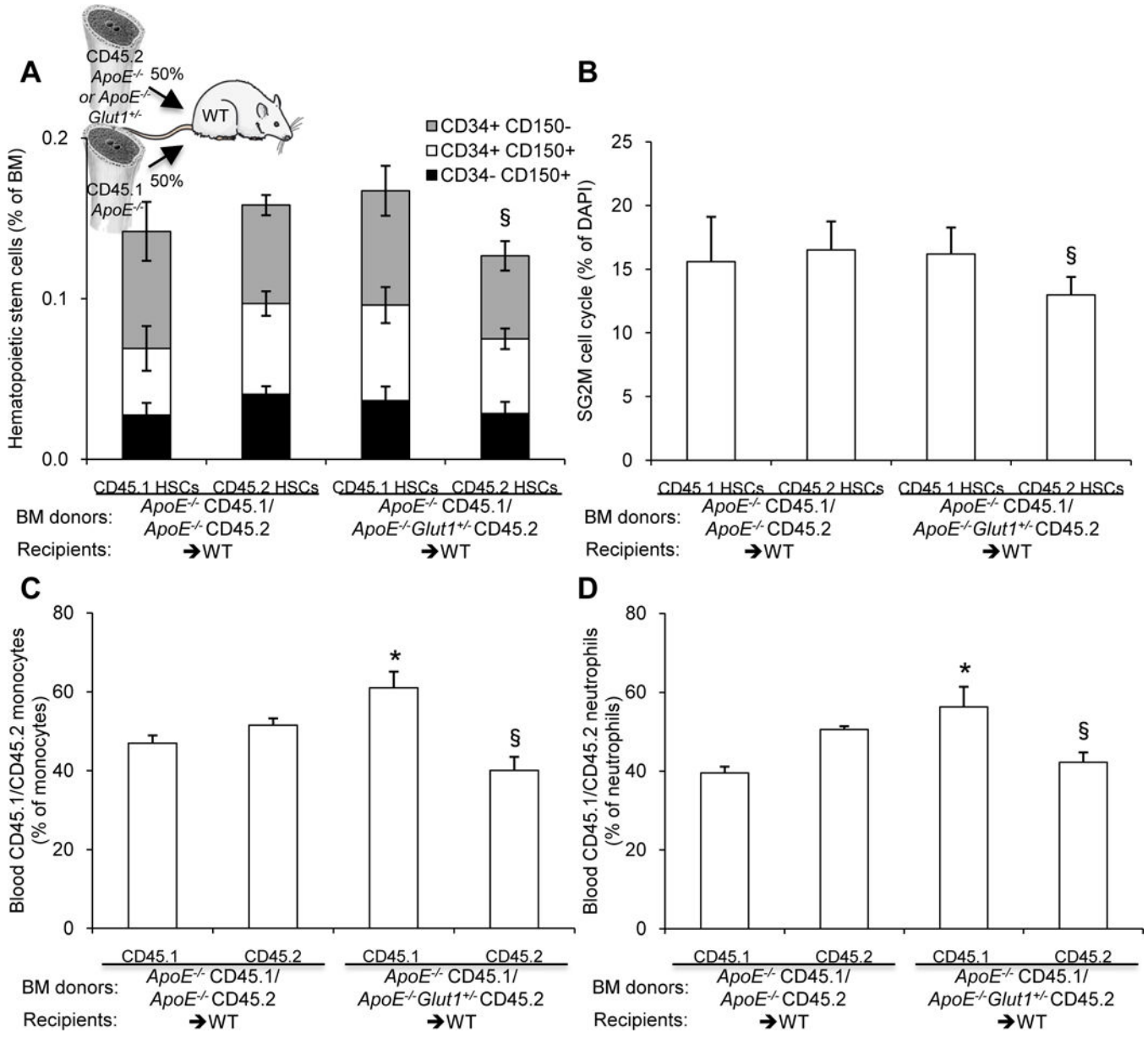

Figure 7. Cell autonomous role of Glut1 on *ApoE*$^{-/-}$ HSPC expansion and myeloid lineage commitment

(A) Schematic diagram showing the protocol for the competitive repopulation assay. Equally mixed portions of BM from the respective genotypes were transplanted into WT recipients. Chow-fed recipient mice were analyzed at 10 weeks after reconstitution by flow cytometry for the contribution of the donor (CD45.1^{+}/CD45.2^{+}) to the HSPC subpopulations from the most quiescent (long-term LT-HSCs) to the most cycling multipotential progenitors (CD34^{-}CD150^{+}>CD34^{+}CD150^{+}> CD34^{+}CD150^{-}) in the bone marrow. **(B)** The percentage of CD45.1^{+} and CD45.2^{+} HSPCs in S/G2M phase was also determined by DAPI staining and flow cytometry in the BM of these mice. The contribution of the donor (CD45.1^{+}/ CD45.2^{+}) to **(C)** the monocytes and **(D)** neutrophils in the peripheral blood was also analyzed. The results are the means ± SEM of 6 to 8 mice per groups. *P<0.05 *vs.* WT mice

receiving CD45.1^{+}*Apoe*$^{-/-}$/CD45.2^{+}*Apoe*$^{-/-}$ mixed BM. $^{\S}P<0.05$ *vs.* CD45.1^{+}*Apoe*$^{-/-}$ cells within the same transplanted mice.

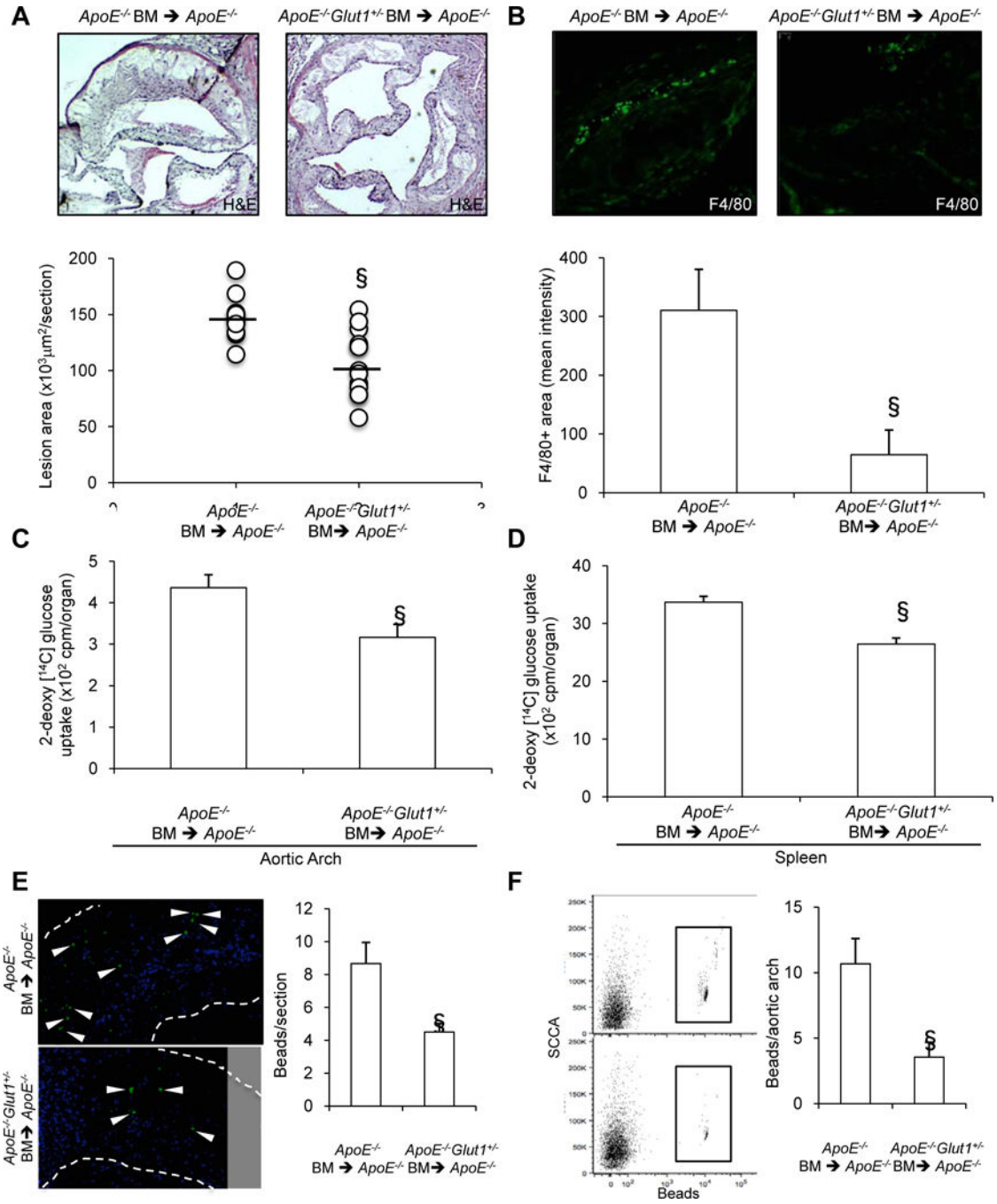

Figure 8. Glut1 deficiency reduces the accelerated atherosclerosis of *ApoE*$^{-/-}$ BM chimeras

(A) Representative hematoxylin and eosin (H&E) staining (magnification, ×100) and quantification by morphometric analysis of the development of atherosclerotic lesions in the proximal aorta of *ApoE*$^{-/-}$ recipient mice transplanted with *ApoE*$^{-/-}$ (n=10) or *ApoE*$^{-/-}$*Glut1*$^{+/-}$ BM that were fed a high fat diet (n=12). The values for individual mice are shown as open circles, representing an average of 6 sections per mouse. The horizontal bars represent the group medians. **(B)** The macrophages were detected by F4/80 immunofluorescent staining in the proximal aorta and quantified as the mean intensity

(magnification, ×200). **(C)** Aortic arch and **(D)** spleen uptake of 2-deoxy-[^{14}C]-glucose in these mice at the end of the study period. All results are the means ± SEM and are representative of 10 to 12 animals per group. **(E–F)** Tracking recruitment of Ly6C^{hi} monocytes in atherosclerotic plaques 2 days after monocyte labeling with green latex beads (n=6). **(E)** Representative pictures (magnification, ×200) and quantification of latex beads (green particles, indicated by arrows) localized within atherosclerotic lesions and expressed as the number of beads per cross section; blue: DAPI-stained nuclei. **(F)** Representative FACS plots and quantification of latex^{+} monocytes that have infiltrated the aortic arch. $^{\S}P<0.05$ *vs.* *ApoE*$^{-/-}$ mice receiving *ApoE*$^{-/-}$ BM.